
Theses and Dissertations

Summer 2011

Measurement of gas evolution from PUNB bonded sand as a function of temperature

Gregory James Samuels
University of Iowa


Copyright 2011 Gregory James Samuels

This thesis is available at Iowa Research Online: <http://ir.uiowa.edu/etd/1260>

Recommended Citation

Samuels, Gregory James. "Measurement of gas evolution from PUNB bonded sand as a function of temperature." MS (Master of Science) thesis, University of Iowa, 2011.
<http://ir.uiowa.edu/etd/1260>.

Follow this and additional works at: <http://ir.uiowa.edu/etd>

 Part of the [Mechanical Engineering Commons](#)

MEASUREMENT OF GAS EVOLUTION FROM PUNB BONDED SAND AS A
FUNCTION OF TEMPERATURE

by

Gregory James Samuels

A thesis submitted in partial fulfillment
of the requirements for the Master of
Science degree in Mechanical Engineering
in the Graduate College of
The University of Iowa

July 2011

Thesis Supervisor: Professor Christoph Beckermann

Graduate College
The University of Iowa
Iowa City, Iowa

CERTIFICATE OF APPROVAL

MASTER'S THESIS

This is to certify that the Master's thesis of

Gregory James Samuels

has been approved by the Examining Committee
for the thesis requirement for the Master of Science
degree in Mechanical Engineering at the July 2011 graduation.

Thesis Committee: _____
Christoph Beckermann, Thesis Supervisor

Pablo Carrica

Albert Ratner

ACKNOWLEDGEMENTS

This work would not have been possible without the support of many people. I would like to express my gratitude to my advisor, Professor Christoph Beckermann, for his tremendous support, guidance, and unwavering insistence that I hold myself to the highest possible standards. I would like to thank the members of my thesis committee, Professors Pablo Carrica and Albert Ratner, for their advice and input. I want to extend thanks to the members of the Solidification Laboratory, especially Kent Carlson, Richard Hardin, and Daniel Galles, for their support and encouragement. I would like thank Peter Hatch of the University of Iowa Department of Chemistry for his advice and expertise in the design and construction of my quartz components. I want to thank Professors Allan Guymon and Gary Aurand of the University of Iowa Department of Chemical and Biochemical Engineering for their insight and generosity in allowing me to use their lab equipment. I extend thanks to Professor Scott Giese of the University of Northern Iowa Department of Industrial Technology for providing additional experimental support. I also thank Jerry Thiel and the students at the University of Northern Iowa Metal Casting Center for their assistance with specimen production. Finally, special thanks are extended to my friends and family, especially my parents David and Joanne and my wife Lindsay, for all their love, support, and understanding during this challenging process.

ABSTRACT

The chemical binders used to make sand molds and cores thermally decompose and release gas when subjected to the high temperature conditions in sand casting processes. Computational models that predict the evolution of the binder gas are being introduced into casting simulations in order to better predict and eliminate gas defects in metal castings. These models require knowledge of the evolved binder gas mass and molecular weight as a function of temperature, but available gas evolution data are limited. In the present study, the mass and molecular weight of gas evolved from PUNB bonded sand are measured as a function of temperature for use with binder gas models. Thermogravimetric analysis of bonded sand is employed to measure the binder gas mass evolution as a function of temperature for heating rates experienced in molds and cores during casting. The volume and pressure of gas evolved from bonded sand are measured as a function of temperature in a specially designed quartz manometer during heating and cooling in a furnace. The results from these experiments are combined with the ideal gas law to determine the binder gas molecular weight as a function of temperature. Thermogravimetric analysis reveals that the PUNB binder significantly decomposes when heated to elevated temperatures, and the PUNB binder gas mass evolution is not strongly influenced by heating rate. During heating of PUNB bonded sand at a rate of $2^{\circ}\text{C}/\text{min}$, the binder gas molecular weight rapidly decreases from 375 g/mol at 115°C to 99.8 g/mol at 200°C . The molecular weight is relatively constant until 270°C , after which it decreases to 47.7 g/mol at 550°C . The molecular weight then steeply decreases to 30.3 g/mol at 585°C and then steeply increases to 47.2 g/mol at 630°C , where it remains constant until 750°C . Above 750°C , the binder gas molecular weight gradually decreases to 33.3 g/mol at 898°C . The present measurements are consistent with the molecular weights calculated using the binder gas composition data from previous studies. The binder gas is composed of incondensable gases above 709°C , and the binder gas partially condenses during cooling at 165°C if the bonded sand is previously heated below 507°C .

TABLE OF CONTENTS

LIST OF TABLES	vi
LIST OF FIGURES	vii
LIST OF NOMENCLATURE	x
CHAPTER	
1. INTRODUCTION	1
1.1 Background and Motivation	1
1.2 Objective of Present Study.....	2
2. LITERATURE REVIEW	3
2.1 Phenolic Urethane Binder Systems.....	3
2.2 Binder Gas Molecular Weight Data.....	4
2.3 Gas Evolution Tests	8
3. EXPERIMENTAL METHODS.....	20
3.1 Experimental Approach of Present Study.....	20
3.2 Preparation of Specimens	20
3.3 Thermogravimetric Analysis	22
3.4 Gas Measurement Apparatus	23
3.5 Metal-Only Expansion Tests.....	25
3.6 Pure Gas Expansion Tests.....	28
3.7 Binder Gas Evolution Tests	31
4. RESULTS AND DISCUSSION.....	39
4.1 Thermogravimetric Analysis	39
4.1.1 Preliminary TGA Measurements	39
4.1.2 Bonded Sand Decomposition Measurements	41
4.1.3 Pure Binder Decomposition Measurements.....	44
4.1.4 Comparison of Bonded Sand and Pure Binder Decomposition Measurements.....	45
4.2 Metal-Only Expansion Measurements during Heating.....	46
4.3 Pure Gas Expansion Measurements during Heating.....	47
4.4 Binder Gas Measurements	51
4.4.1 Binder Gas Evolution during Heating and Cooling.....	51
4.4.2 Effects of Hydrogen Dissolution on the Binder Gas Molecular Weight Measurements	54
4.4.3 Effects of Sand Expansion on the Binder Gas Molecular Weight Measurements	56
4.4.4 Additional Analysis of the Measured Peak in the Binder Gas Molecular Weight during Heating	56
4.4.5 Molar Evolution of the Binder Gas during Heating and Cooling.....	57
4.4.6 Comparison of the Present Molecular Weight Measurements with the Results from Previous Studies.....	58

5. CONCLUSIONS.....	86
REFERENCES	88

LIST OF TABLES

Table

1. Time-averaged mass fraction and mixture molecular weight of gas components evolved from PUCB and PUNB bonded sand within 2 minutes after pouring during the experiments of Bates *et al.* and Scott *et al.*.....14
2. Primary chemical components identified by McKinley *et al.* and Lytle through GC-MS analysis during 20 seconds of pyrolysis of 1.5% PUCB bonded sand and the calculated gas mixture molecular weights15
3. Chemical components identified by Wang *et al.* through GC-FID and GC-TCD analysis during TGA pyrolysis of 1.5% PUCB bonded sand at a heating rate of 10°C/min and the calculated gas mixture molecular weight16
4. Piecewise polynomial fitted to the measurements of the fraction of original binder mass remaining in bonded sand samples during TGA pyrolysis at a heating rate of 2°C/min with a total argon flow rate of 25 cm³/min.....66
5. Primary sources of error in the binder gas molecular weight measurements80
6. Piecewise polynomial fitted to the binder gas molecular weight measurements obtained during heating of PUNB bonded sand samples at a rate of 2°C/min.....85

LIST OF FIGURES

Figure

1. General bonding reaction equation for PUCB or PUNB binder systems	12
2. Experimental technique used by Bates and Monroe to sample the gas evolved from decomposition of bonded sand during pouring of metal castings.....	13
3. Gas evolution tester employed by Zhang <i>et al.</i>	17
4. Experimental methods employed by Bates and Monroe to measure the (a) volume and (b) pressure of gas evolved from bonded sand.....	18
5. Techniques for measuring binder gas evolution from cores immersed in molten metal.....	19
6. Schematic of gas measurement apparatus and important geometric quantities	35
7. Procedure for filling GED with only liquid metal	36
8. Procedure for filling GED with a gas sample and liquid metal	37
9. Procedure for filling GED with a PUNB bonded sand sample and liquid metal.....	38
10. Measured change in mass as a function of temperature typical of PUNB bonded sand samples, pure IC55 silica sand samples, the empty sample pan, and quartz rods during heating at a rate of 100°C/min with a total argon gas flow of 80 cm ³ /min	60
11. Measured change in the mass of quartz rods as a function of temperature during heating at rates of 2°C/min, 10°C/min, and 100°C/min	61
12. Comparison of the uncorrected and corrected percentage of mass remaining as a function of temperature in a (a) 55 mg PUNB bonded sand samples and (b) 7.5 mg pure PUNB binder samples during heating at a rate of 100°C/min with a total argon gas flow of 80 cm ³ /min	62
13. Measured percentage of mass remaining in the individual components of PUNB bonded sand as a function of temperature during heating at a rate of 100°C/min with a total argon gas flow of 80 cm ³ /min	63
14. Measured fraction of original binder mass remaining in various masses of PUNB bonded sand as a function of temperature during heating at a rate of 100°C/min with a total argon gas flow of 80 cm ³ /min	64
15. Measured fraction of original binder mass remaining in 55 mg PUNB bonded sand samples as a function of temperature during heating at rates of 2°C/min, 10°C/min, and 100°C/min with total argon gas flow rates of (a) 80 cm ³ /min and (b) 25 cm ³ /min	65

16. Comparison of the fraction of original binder mass remaining in bonded sand samples as a function of temperature during heating from the present PUNB measurements (averaged) using total argon flow rates of (a) 80 cm ³ /min and (b) 25 cm ³ /min with the fractions calculated from TGA data of previous studies.....	67
17. Measured fraction of original binder mass remaining in 7.5 mg pure PUNB binder samples as a function of temperature during heating at rates of 2°C/min, 10°C/min, and 100°C/min with total argon gas flow rates of (a) 80 cm ³ /min and (b) 25 cm ³ /min.....	68
18. Comparison of the fraction of original binder mass remaining in pure binder samples as a function of temperature during heating from the present PUNB measurements (averaged) using total argon gas flow rates of (a) 80 cm ³ /min and (b) 25 cm ³ /min with the fraction calculated from TGA data of Lytle for pure PUCB binder with a 55:45 ratio of Part 1 to Part 2.....	69
19. Comparison of the average fraction of original binder mass remaining in 55 mg PUNB bonded sand and 7.5 mg pure PUNB binder samples as a function of temperature during heating at rates of 2°C/min, 10°C/min, and 100°C/min with total argon gas flow rates of (a) 80 cm ³ /min and (b) 25 cm ³ /min.....	70
20. Measured metal-only height change in the GED as a function of temperature during heating at constant rates ranging from 2°C/min to 15°C/min.....	71
21. Liquid metal volumetric expansion coefficients calculated from metal-only expansion in the GED and the borosilicate bulb as a function of temperature during heating.....	72
22. Comparison of measured and predicted metal-only height change in the GED as a function of temperature during heating.....	73
23. Measured height change as a function of temperature for all pure gas expansion tests in the GED.....	74
24. Measured temperature difference in the GED's thermocouple wells as a function of metal temperature for all pure gas expansion tests.....	75
25. Ratio of measured to known molecular weight of (a) argon gas and (b) hydrogen gas as a function of temperature during heating.....	76
26. Ratio of measured to known molecular weight of argon gas from all pure argon gas expansion tests as a function of temperature.....	77
27. Measured height change as a function of temperature during heating and cooling of different PUNB bonded sand sample masses.....	78
28. Binder gas molecular weight measurements as a function of temperature during heating and cooling of different PUNB bonded sand sample masses.....	79

29. Comparison of the measured binder gas molecular weight as a function of temperature with and without the hydrogen dissolution correction during heating of a 0.637 g PUNB bonded sand sample at a rate of 2°C/min	81
30. Comparison of the measured to known molecular weight ratio of argon for pure argon gas samples and argon gas with a 1.018 g sample of cleaned IC55 silica sand as a function of temperature during heating.....	82
31. Measured binder gas moles evolved per original binder mass as a function of temperature during heating and cooling of different PUNB bonded sand sample masses.....	83
32. Comparison of the piecewise polynomial fitted to the present binder gas molecular weight measurements for a heating rate of 2°C/min with the results from previous studies as a function of temperature.....	84

LIST OF NOMENCLATURE

Acronyms

BIO	Black Iron Oxide
DSC	Differential Scanning Calorimetry
GC	Gas Chromatography
GC-FID	Gas Chromatography-Flame Ionization Detector
GC-MS	Gas Chromatography-Mass Spectrometry
GC-TCD	Gas Chromatography-Thermal Conductivity Detector
GED	Gas Evolution Device
HC _{total}	Total Hydrocarbons
PU	Phenolic Urethane
PUCB	Phenolic Urethane Cold-Box
PUNB	Phenolic Urethane No-Bake
TGA	Thermogravimetric Analysis
TGA-MS	Thermogravimetric Analysis-Mass Spectrometry

Symbols

β_m	volumetric expansion coefficient of the liquid metal (1/°C)
β_m^{con}	volumetric expansion coefficient of the liquid that is constant with respect to temperature (1/°C)
β_m^{eff}	effective volumetric expansion coefficient of the liquid metal in the GED (1/°C)
φ	ratio of the measured to known molecular weight of an ideal gas
ρ_m	density of the liquid metal (g/cm ³)
ρ_m^0	density of the liquid metal at room temperature (g/cm ³)
χ	sample binder content based on total sample weight (wt. %)
$D_{1,eff}$	effective internal diameter of cylinder 1 of the GED (cm)
D_2	internal diameter of cylinder 2 of the GED (cm)
f	fraction of original binder mass remaining

g	gravitational acceleration (m/s ²)
Δh_1	measured total metal height change in cylinder 1 of the GED (cm)
Δh_2	measured total metal height change in cylinder 2 of the GED (cm)
Δh_2^c	total metal height change in cylinder 2 of the GED that includes a correction for hydrogen gas dissolution into the liquid metal (cm)
Δh_2^g	the portion of height change in cylinder 2 of the GED due to gas evolution and/or expansion (cm)
ΔH	height difference between the metal surfaces in cylinders 1 and 2 of the GED (cm)
h_1^0	initial liquid metal height in cylinder 1 of the GED (cm)
h_2^0	initial liquid metal height in cylinder 2 of the GED (cm)
m_b	total mass of evolved binder gas (g)
m_g	total gas mass (g)
m_g^d	mass of hydrogen gas dissolved into the liquid metal (g)
m_g^{d*}	mass of hydrogen gas dissolved into the liquid metal that is approximated by a Taylor series (g)
m_m	mass of liquid metal in the filled GED (g)
m_s	sample mass measured by the TGA machine (g)
m_s^0	total initial sample mass loaded into the TGA machine or the GED (g)
M_{Ar}	molecular weight of argon gas (g/mol)
M_b	molecular weight of the evolved binder gas (g/mol)
M_{H_2}	molecular weight of hydrogen gas (g/mol)
M_i	true molecular weight of a measured gas i (g/mol)
M_g	molecular weight of an ideal gas component or gas mixture (g/mol)
n_b	moles of evolved binder gas per original binder mass (mol/g)
P_{atm}	atmospheric pressure (Pa)
P_g	gas pressure (Pa)
P_g^0	initial gas pressure (Pa)
P_{probe}	pressure from the weight of the displacement probe and boat (Pa)

\bar{R}	universal gas constant (J/mol/K)
ΔT	difference between the measured glass and metal temperatures (°C)
T	gas or sample temperature
T^0	initial gas or sample temperature
T_{glass}	measured exterior glass temperature (°C)
T_m	measured metal temperature (°C)
T_m^0	measured initial metal temperature (°C)
\dot{T}	heating rate (°C/min)
V_{fill}^0	volume contained by the filled GED at the initial temperature (cm ³)
V_g	gas volume (cm ³)
V_g^0	initial gas volume (cm ³)
ΔV_g	change in gas volume (cm ³)
ΔV_m	change in volume of the liquid metal (cm ³)

CHAPTER 1. INTRODUCTION

1.1 Background and Motivation

Modern foundries use nonpermanent molds and cores that are made from silica sand and held together by a resin binder to maintain the desired casting shape until the metal is poured and solidified. The bonded sand mold creates the primary form of the casting, and bonded sand cores are employed to produce cavities within the casting. A great deal of heat is transferred to the sand and resin binder when the molten metal is poured into the mold. This causes the binder to pyrolyze, or thermally decompose at elevated temperatures in the absence of oxygen, and a significant amount of gas evolves when the binder degrades [1]. Binder gas evolution, or simply the characteristic production of gas due to binder thermal decomposition, may be discussed in terms of the generation of binder gas mass or volume.

It is well understood that binder gas evolution can profoundly influence the quality of metal castings [2-4]. Inadequate venting of the binder gas from the mold and employed cores will increase the tendency to form casting porosity defects, which are gas bubbles that become trapped in the metal during solidification [1]. The two types of porosity defects most commonly associated with binder gas evolution are blowholes and pinholes [5-9]. The evolved binder gas will penetrate the molten metal's surface if the gas pressure exceeds the local metallostatic pressure, which causes blowholes to form if the gas does not escape from the metal before solidification occurs [1,9]. The solubility of gas in the liquid metal decreases as the metal solidifies, and pinholes form when dissolved gas is rejected from solution and trapped in the metal during solidification. Binder gas generation at the mold-metal interface (defined here as the locations where the mold or core contact the metal) may lead to increased dissolution of gas in the metal, thereby increasing the tendency for pinholes to form as the liquid metal solidifies [1,9].

Bonded sand molds and cores are permeable and may have porosities as high as 50% [9]. The gas evolved in the mold usually has ample opportunity to diffuse away

from the mold-metal interface through the porous space in the mold. However, gas defects may still form due to the binder gas generation in the mold. In the case of cores, the area of the core prints (insets in the mold for holding cores in place) provides the only means for the gas to escape the cores without passing through the liquid metal. In addition, a sand core is heated much faster than the mold (causing more complete binder decomposition and greater gas evolution in the core) because the core is typically surrounded on many sides by hot metal and the core is much smaller compared to the mold [1]. Many variables influence the formation of gas defects in castings; however, the conditions that promote the formation of binder gas defects during casting are more often found in cores than in the mold. Defects caused by binder gas evolution result in large amounts of scrap and are of great concern to the metal casting industry.

In response to these issues, computational models that predict binder gas evolution during casting have been incorporated into metal casting simulations in order to better predict the occurrence of gas defects (for example, References [10-12]). Accurate prediction of such defects allows for better design of sand molds and cores for the production of quality castings. Crucial elements required for the use and validation of binder gas evolution models are the mass and molecular weight of the evolved gas as a function of temperature. Unfortunately, temperature-resolved binder gas mass evolution and molecular weight data corresponding to the conditions experienced during sand casting processes are extremely limited.

1.2 Objective of Present Study

The objective of this study is to measure the mass and molecular weight of the gas evolved during decomposition of phenolic urethane no-bake bonded sand as a function of temperature at conditions similar to those experienced during actual sand casting processes. The experimental results will provide improved input and validation data for binder gas evolution models used in casting simulations.

CHAPTER 2. LITERATURE REVIEW

2.1 Phenolic Urethane Binder Systems

A wide variety of chemical binder systems are available for the production of molds and cores used in the sand casting process. The phenolic urethane (PU) system is the most commonly used synthetic binder system in the United States [13]. The PU binder system is a three-part system that combines a phenol-formaldehyde resin dissolved in solvents (Part 1), a polymeric isocyanate dissolved in solvents (Part 2), and a tertiary amine catalyst (Part 3) to produce a urethane bond. The general reaction equation for the PU system can be seen in Figure 1. The solvents are employed to reduce the viscosity and increase the reactivity of the binder components [13,14]. The catalyst acts to control and accelerate the reaction between the phenolic resin and the isocyanate [13].

The PU system can be further divided into phenolic urethane cold-box (PUCB) and phenolic urethane no-bake (PUNB) processes, with the primary difference between these methods being the manner in which the catalyst is introduced to the system. The PUCB process involves coating sand with the Part 1 and Part 2 components, shaping and compacting the sand-binder mixture into the desired form, vaporizing the Part 3 catalyst and blowing it through the sand-binder mixture, and blowing air through the bonded sand to remove any residual gaseous catalyst. The PUNB process involves combining the Part 1 component with the Part 3 catalyst as a liquid, coating the sand with the resin-catalyst mixture, adding the Part 2 component to the coated sand, shaping and compacting the sand-binder mixture into the desired form, and allowing the bonded sand to cure. The PUCB catalyst is designed to function primarily as a reaction accelerant, while the PUNB catalyst acts to predictably control and accelerate the bonding reaction [15,16].

The chemical formulations employed in Parts 1-3 for the PUCB and PUNB processes are different. This is mainly due to the difference in which the catalyst is added to the sand-binder mixture. However, the PUCB and PUNB systems are based on the same urethane bonding chemistry illustrated in Figure 1 [13,14]. This similarity allows

the composition and molecular weight of the gas evolved from these systems to be reasonably compared.

2.2 Binder Gas Molecular Weight Data

Knowledge of the evolved binder gas composition facilitates determination of the gas's molecular weight. Unfortunately, however, temperature-resolved binder gas composition data are quite limited.

Early studies by Bates and Scott [17,18], Bates and Monroe [19], and Scott *et al.* [20] involved pouring aluminum, gray iron, and steel into molds made using different binder systems and periodically sampling the gas generated at the mold-metal interface. The experimental setup used to sample the gas in Reference [19] is illustrated in Figure 2, and this method was essentially the same as those employed in References [17], [18], and [20]. Bonded sand was rammed inside a Büchner funnel fitted with a vent tube, and the funnel was rammed into the drag of the sand mold. The inlet of the vent tube was positioned to be 6.35 mm (0.25 in) from the mold-metal interface. The opposite end of the tube was attached to a hypodermic needle. Once the casting was poured, gas evolved from the bonded sand inside the funnel, and the binder gas was sampled by inserting evacuated glass tubes into the vent tube's hypodermic needle. The gas samples were analyzed by gas chromatography (GC) coupled with either a flame ionization detector (GC-FID) or a thermal conductivity detector (GC-TCD) to determine the volume concentrations (%*V/V*) of hydrogen, oxygen, nitrogen, carbon monoxide, carbon dioxide, and the total hydrocarbons (HC_{total}) in the binder gas. HC_{total} was measured as the equivalent concentration of methane. The average composition and mixture molecular weight of the gas evolved within two minutes after pouring metal into PUCB and PUNB bonded sand molds are shown in Table 1. The reported volume concentrations are converted to mass fractions for the present analysis. The molecular weights calculated from the average gas compositions within the first two minutes after pouring should

roughly correspond to the pouring temperatures of the metal [21]. The results in Table 1 show that in general the binder gas generated during pouring of the gray iron and steel castings was mostly comprised of carbon monoxide and carbon dioxide, had varying amounts of nitrogen and hydrocarbons, and low amounts of hydrogen and oxygen. The binder gas from the aluminum castings, poured at significantly lower temperatures than the gray iron and steel castings, was comprised almost entirely of oxygen and nitrogen. This indicates that the evolution of binder gas within the first two minutes after pouring the aluminum castings was insufficient to replace the air atmosphere originally in the molds, implying that hydrogen, carbon monoxide, carbon dioxide, and hydrocarbons significantly evolve at higher temperatures. Unfortunately, the binder gas likely experienced some condensation before it escaped the test mold and was collected, making the measured composition not entirely representative of the actual binder gas composition. In addition, the binder gas samples had the opportunity to cool inside the collection tubes prior to injection of the samples into the gas chromatograph, which likely caused the binder gas to condense before it could be analyzed. Regardless of these issues, the molecular weight data calculated from References [17-20] are useful for comparison against the present molecular weight measurements.

More recently, McKinley *et al.* [22] (with detailed information and analysis available in the work of Lytle [23]) performed flash pyrolysis of 1.5% PUCB bonded sand and used gas chromatography-mass spectrometry (GC-MS) to analyze the evolved binder gas. 100 mg samples of PUCB bonded sand were rapidly heated to 500, 700, and 900°C in a helium atmosphere and held at these temperatures for various periods of time. The pyrolysis products were swept directly into the gas chromatograph, and gas species ranging from 10 g/mol to 425 g/mol were detected by the mass spectrometer. The mass fraction of the primary components emitted from the PUCB bonded sand during 20 seconds of pyrolysis at 700°C and 900°C and the mixture molecular weights calculated from the composition data are shown in Table 2. The components in Table 2 comprise

more than 99% of the measured gas species at each temperature, with the remaining gases being high molecular weight compounds. It can be seen from Table 2 that, besides carbon monoxide, the major species evolved are hydrocarbons. In addition, the binder gas composition experiences significant changes between 700°C and 900°C. None of the components listed in Table 2 were detected during pyrolysis at 500°C. However, the molecular weight of the gas mixture evolved at 500°C was calculated to be 137 g/mol. The gas components evolved from bonded sand will freely mix throughout the casting process, and Reference [22] acknowledges that the evolved binder gas components will interact with one another and may combine to form new compounds. Therefore, the gas species separation required for thorough GC analysis deviates from the conditions experienced during actual casting processes. Despite this fact, the detailed composition data from References [22] and [23] currently provide the only means to directly obtain temperature-resolved molecular weight data for gas evolved from bonded sand used in casting processes.

Very recently, Wang *et al.* [24] performed pyrolysis of 1.5% PUCB bonded sand in a thermogravimetric analyzer from 20°C to 900°C at a heating rate of 10°C/min with a total nitrogen gas flow rate of 60 cm³/min. Granular activated carbon tubes and Tedlar[®] gas sampling bags were used to collect the binder gas from the analyzer throughout the heating process. The contents of the granular activated carbon tubes were analyzed by GC-FID, and the contents of the gas sampling bags were analyzed by both GC-FID and GC-TCD. Separate thermogravimetric analysis (TGA) experiments were employed to measure the mass loss in PUCB bonded sand from thermal decomposition, which is equivalent to the evolved binder gas mass. Unfortunately, the components detected in the binder gas evolved from bonded sand during TGA pyrolysis only accounted for 21% of the generated binder gas mass. The investigators reported that significant amounts of liquid pyrolysis products collected within the TGA machine, thereby preventing these compounds from being analyzed. As in References [17-20], the analysis of the gas was

performed well after the gas was collected, which may have caused additional error in the measurement of the gas composition. The mass fractions of the measured components emitted from the PUCB bonded sand (relative to the total generated binder gas mass measured from TGA of bonded sand) and the corresponding gas mixture molecular weight are shown in Table 3. The calculated molecular weight is not particularly useful because it represents only a small portion of the gas components evolved from the bonded sand. In addition, the calculated molecular weight is not temperature-resolved, which prevents it from being directly compared with the present binder gas molecular weight measurements. Reference [24] also performed TGA pyrolysis coupled with mass spectrometry (TGA-MS) to determine the temperatures at which major binder gas components evolved. Again, however, condensation of the binder gas likely prevented this analysis method from fully characterizing the binder gas molecular weight as a function of temperature.

Comparison of the results from Tables 1 through 3 offers additional insight into the nature of the binder gas evolution for PU systems. References [23] and [24] did not detect any oxygen or nitrogen in the binder gas. Therefore, it seems quite plausible that the nitrogen and oxygen measured in References [17-20] during all casting experiments were actually from the residual air in the mold. The significant hydrocarbon content at 700°C reported by References [22] and [23] also contradicts the results of References [17-20] at 750°C (aluminum castings). In addition, the uncharacterized portion of the binder gas mass (79% of the total evolved gas mass) in Reference [24] most likely contained complex hydrocarbons and other organic compounds. There is agreement between the previous studies on the presence (although not the relative quantity) of carbon monoxide and methane in the binder gas. References [17-20] and [24] agree on the presence (though again not the relative quantity) of carbon dioxide in the binder gas. It should also be noted that the gas mixture molecular weights calculated from the composition data from previous studies are relatively similar in magnitude.

Even though coupling GC with any one of the many types of gas detectors provides the means to analytically determine the binder gas composition and molecular weight, this technique is not well suited to generate the magnitude of temperature-resolved molecular weight data required in binder gas models. TGA coupled with a gas detector allows for more reasonable measurement of the gas composition (or the gas molecular weight when TGA-MS is employed) as a function of temperature. As exemplified by the TGA and GC experiments in Reference [24], however, condensation of the binder gas prior to analysis may dramatically affect the binder gas measurements. Elimination of binder gas condensation from the TGA system likely requires complex modification of the analysis equipment, which is undesirable.

2.3 Gas Evolution Tests

Determination of the binder gas molecular weight as a function of temperature from additional binder gas composition measurements is impractical due to the previously described experimental difficulties, analysis complexity, and high equipment costs. The second method for determining the binder gas molecular weight is to use the ideal gas law in conjunction with measurements of the evolved binder gas mass, volume, and pressure as a function of temperature. TGA of bonded sand facilitates determination of the binder gas mass evolution as a function of temperature. The experimental difficulty lies in measuring the volume and pressure of the evolved gas as a function of temperature under conditions similar to those experienced during actual casting processes.

Dietert *et al.* [25], Moore and Mason [26] and Zhang *et al.* [27] used similar apparatuses to measure the pressure generated by gas evolved from bonded sand heated in a furnace. The gas pressure could then be converted to gas volume by a calibration method. The device's interior surfaces were maintained above 110°C to limit gas condensation and the bonded sand samples were immersed in a nitrogen atmosphere during the test. The device used by Reference [27] is shown in Figure 3. Unfortunately,

many issues prevent such a device from being used to measure the molecular weight of the binder gas. The apparatus only allows tests to be performed at individual furnace temperatures, which severely limits the experimental flexibility of the molecular weight measurements. Only a portion of the evolved gas volume was contained within the hot zone of the furnace, and this will likely cause nonisothermality in the evolved gas volume that would lead to inaccurate volume and pressure measurements. Furthermore, heating the gas evolution system's interior surfaces to 110°C may not be sufficient to prevent condensation of all the binder gas components. The binder gas mass measurements from the TGA experiments need to be matched with the evolved gas volume and pressure measurements as a function of temperature for use in the molecular weight calculations, but the device offers no means to directly measure the temperature of the bonded sand and evolved binder gas. In addition, the heating rates employed during measurement of the evolved binder gas mass, volume, and pressure as a function of temperature need to be the same in order to properly calculate the binder gas molecular weight. The gas evolution system does not provide the means to control the heating rate of the bonded sand and evolved binder gas, which makes volume and pressure measurements obtained with the device unsuitable for the molecular weight calculations. The gas evolution system employed in References [25-27] must undergo significant modifications before it could be used to measure the binder gas volume, pressure, and temperature for use in binder gas molecular weight calculations.

In addition to analyzing the binder gas composition, Bates and Monroe [19] measured the volume and pressure of gas evolved from the mold during pouring of gray iron, steel, and aluminum castings. Their experimental methods for measuring the binder gas volume and pressure are shown in Figure 4. Separate funnels attached to vent tubes and filled with test sand were rammed into the sand mold in a similar manner as those employed for gas sampling as previously described. One vent tube was attached to the inlet of a bubble flow meter, and the other vent tube was connected to a pressure

transducer. After the casting was poured, the evolved gas volume was measured by monitoring the movement of bubbles through the bubble flow meter, and the gas pressure was directly measured with the pressure transducer. A thermocouple protected by a quartz sheath was also used to measure the temperature at the center of the casting. These experimental methods have limited use in the present study. Even with modification, this approach does not easily facilitate the measurement of the gas volume and pressure at the same location inside the bonded sand sample. The temperature of the binder gas at the inlet points of the vent tubes also needs to be measured. The bonded sand sample likely needs to be fairly large to accommodate both vent tubes as well as a temperature probe. The tendency for the binder gas to condense in the bonded sand will increase as the bonded sand sample size increases, and binder gas condensation must be avoided in order to properly measure the binder gas molecular weight. Nonisothermality in the evolved gas along the length of the vent tube attached to the bubble flow meter may lead to erroneous volume readings. Another problem is that the heating rate of the bonded sand and evolved binder gas cannot be controlled, and this is highly undesirable for reasons previously described. While it is valuable to study gas evolution characteristics during actual casting processes, the experimental approach of Reference [19] is impractical for measuring the binder gas molecular weight as a function of temperature.

Scarber *et al.* [28] developed an apparatus for measuring the gas evolution rates and evolved gas volumes in cores immersed in molten metal. This apparatus is illustrated in Figure 5 (a). A cylindrical bonded sand core was printed on a sealed steel holder attached to a preheated gas line. The core was then immersed in molten metal. The gases produced from binder decomposition flowed out of the core through the gas line and displaced oil in a preheated chamber. The displaced oil flowed out of the chamber through a vent tube and into a container positioned on a precision electronic balance. Knowledge of the oil density and the measured oil weight facilitated calculation of the evolved volume of binder gas. The gas line and oil chambers were maintained at

temperatures that would prevent water condensation, and thermocouples monitored the temperatures in the gas line. Winardi *et al.* [29] inserted a pressure probe into the axial center of the core to measure the gas pressure inside the core during molten metal immersion. Their device is depicted in Figure 5 (b). Winardi *et al.* [30] later replaced the pressure probe with thermocouple probes inserted at various distances from the interface of the core and the metal. Starobin *et al.* [12] used the gas pressure and total collected gas volume data from the previously described core immersion experiments to calculate an effective binder gas molecular weight. The calculated value of 23 g/mol from Reference [12] is in agreement with the gas composition results of References [17-20], but this value only applies to the entire volume of evolved binder gas and is unrelated to the binder gas temperature. Like all previous gas evolution measurement techniques, the core immersion apparatus described by Reference [28] may still allow the binder gas to condense. Even though many volatiles with low boiling points and water vapor are kept from condensing due to the preheating of the gas line and oil chamber, volatiles with high boiling points may still be allowed to condense within the core itself, the gas lines, or in the oil chamber. The inherent design of the apparatus may cause delays between the evolution of binder gas and the corresponding volume measurement by oil displacement. Combining the experimental techniques of References [29] and [30] allows for measurement of the binder gas volume and pressure as a function of temperature, but the volume measurement occurs at a location apart from the pressure and temperature measurements. Ideal determination of the binder gas molecular weight requires measurement of the volume of gas evolved from the bonded sand while simultaneously measuring the pressure and temperature of that same evolved gas volume. The lack of control over the heating rates in the core will greatly complicate the measurement of the binder gas molecular weight for reasons previously described. Therefore, the core immersion apparatus is not suitable for measuring the binder gas molecular weight as a function of temperature.

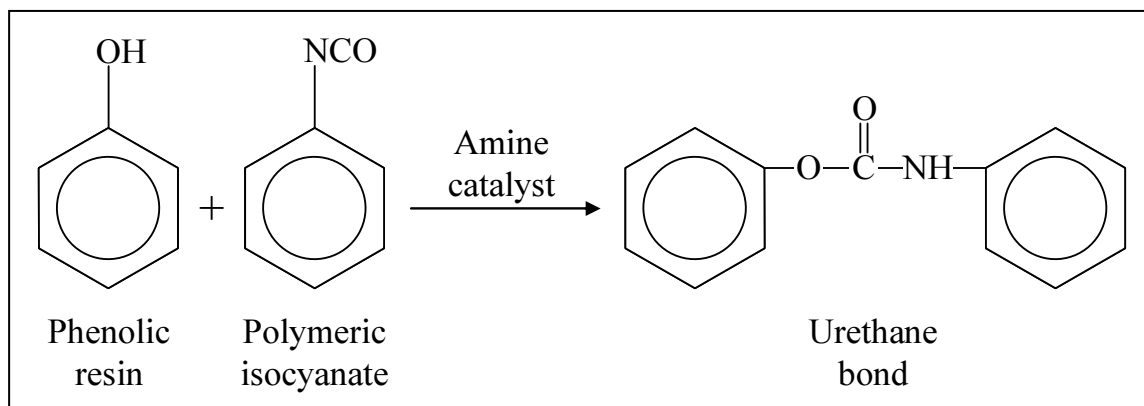


Figure 1: General bonding reaction equation for PUCB or PUNB binder systems [13].

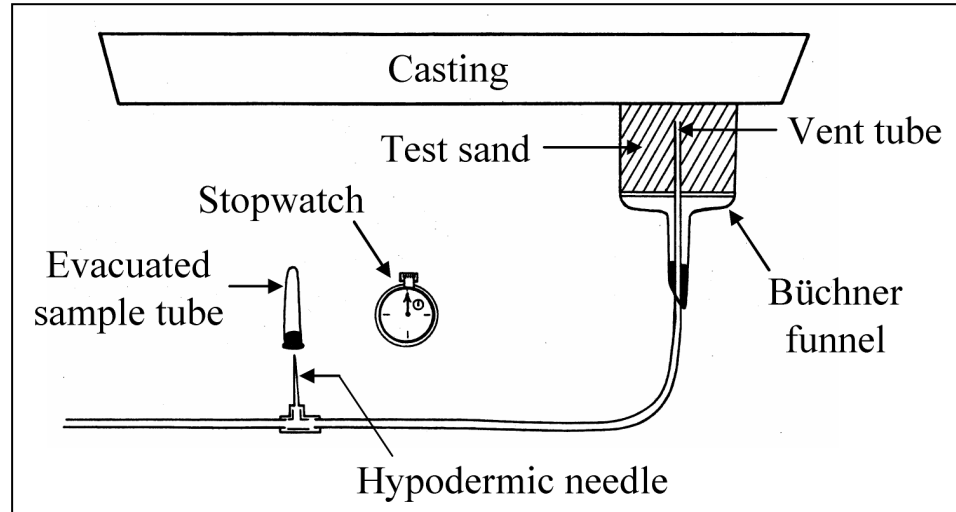


Figure 2: Experimental technique used by Bates and Monroe [19] to sample the gas evolved from decomposition of bonded sand during pouring of metal castings. The other sections of the casting's mold are not illustrated. This sampling method is essentially the same as those employed by Bates *et al.* [17,18] and Scott *et al.* [20].

Table 1: Time-averaged mass fraction and mixture molecular weight of gas components evolved from PUCB and PUNB bonded sand within 2 minutes after pouring during the experiments of Bates *et al.* [17-19] and Scott *et al.* [20].

Experiment Description		Component Mass Fraction						Mixture Molecular Weight [g/mol]
Binder System	Metal and Average Pouring Temperature	H ₂	O ₂	N ₂	CO	CO ₂	HC _{total} *	
2% PUCB	Gray Iron at 1446°C	0.068	0.013	0.041	0.367	0.371	0.140	15
1.3% PUCB	Gray Iron at 1457°C	0.071	0.038	0.160	0.37	0.25	0.11	15
2% PUNB	Gray Iron at 1431°C	0.066	0.01	0.05	0.35	0.38	0.15	15
2% PUNB	Gray Iron at 1430°C	0.037	0.086	0.297	0.202	0.318	0.061	20
2% PUNB	Steel at 1620°C	0.050	0.066	0.244	0.404	0.215	0.020	18
2% PUNB	Aluminum at 750°C	0.0002	0.208	0.7288	0.0039	0.057	0.0018	29

*Total hydrocarbons measured as equivalent to methane

Table 2: Primary chemical components identified by McKinley *et al.* [22] and Lytle [23] through GC-MS analysis during 20 seconds of pyrolysis of 1.5% PUCB bonded sand and the calculated gas mixture molecular weights.

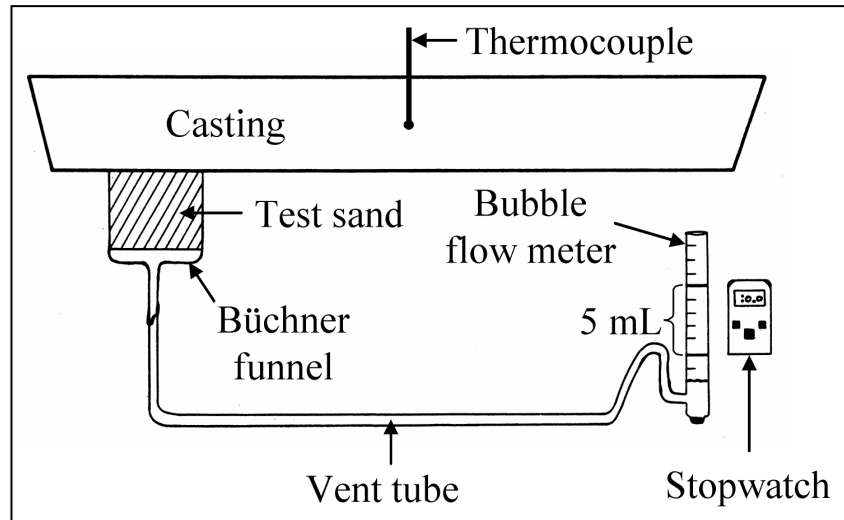
Component	Chemical Formula	Mass Fraction at 700°C	Mass Fraction at 900°C
Methane	CH ₄	0.0881	0.0701
Carbon Monoxide	CO	0.2311	0.1243
Ethene	C ₂ H ₄	0.0523	0.1008
Propene	C ₃ H ₆	0.2053	0.3047
2-Propenenitrile	C ₃ H ₃ N	0.0000	0.0239
1,3-Butadiene	C ₄ H ₆	0.0638	0.0921
1-Butene	C ₄ H ₈	0.1816	0.1152
1,3-Pentadiene	C ₅ H ₈	0.0590	0.0967
1-Pentene	C ₅ H ₁₀	0.1118	0.0708
Mixture Molecular Weight of Primary Components [g/mol]:		36.3 at 700°C	38.00 at 900°C

Table 3: Chemical components identified by Wang *et al.* [24] through GC-FID and GC-TCD analysis during TGA pyrolysis of 1.5% PUCB bonded sand at a heating rate of 10°C/min and the calculated gas mixture molecular weight.

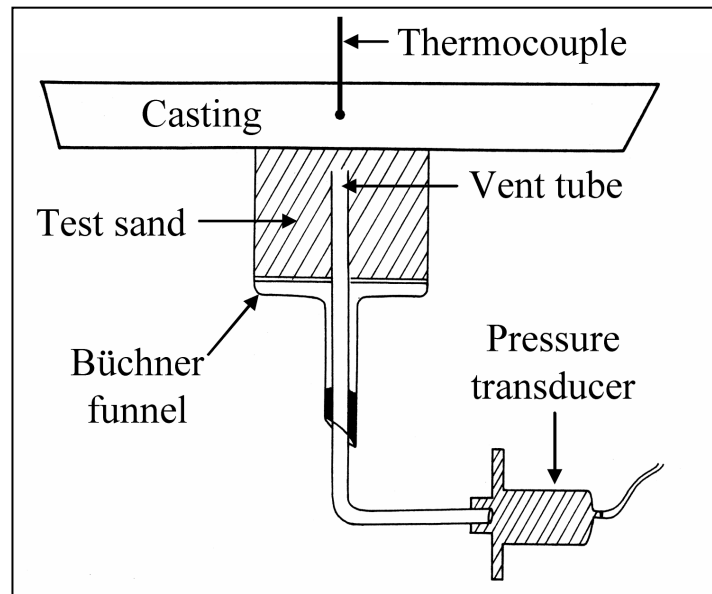
Component	Chemical Formula	Mass Fraction from 20°C to 900°C
Methane	CH ₄	0.0243
Carbon Monoxide	CO	0.0287
Carbon Dioxide	CO ₂	0.1081
Hexane	C ₆ H ₁₄	0.0004
Benzene	C ₆ H ₆	0.0016
Toluene	C ₇ H ₈	0.0026
Xylene	C ₈ H ₁₀	0.0015
Phenol	C ₆ H ₆ O	0.0042
Cresols	C ₇ H ₈ O	0.0030
Methylnaphthalene	C ₁₁ H ₁₀	0.0019
Methyl Oleate	C ₁₉ H ₃₆ O ₂	0.0117
Other Species [*]	–	0.0188
*Measured as equivalent to methyl oleate		
Mixture Molecular Weight of Measured Components [g/mol]:		38.7 from 20°C to 900°C



Figure 3: Gas evolution tester employed by Zhang *et al.* [27]. Dietert *et al.* [25] and Moore and Mason [26] employed similar devices to study gas evolution from bonded sand. The illustration was obtained from Reference [31].

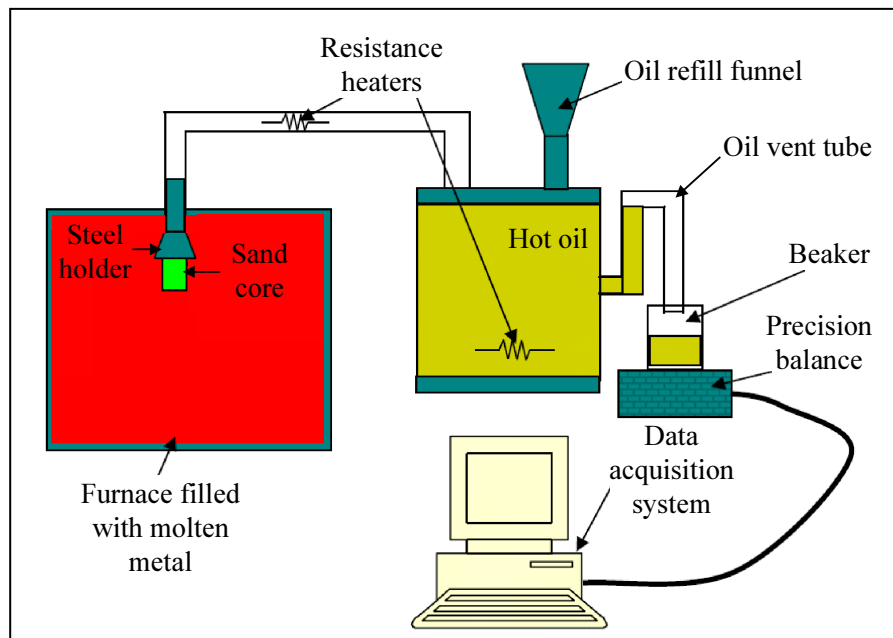


(a)

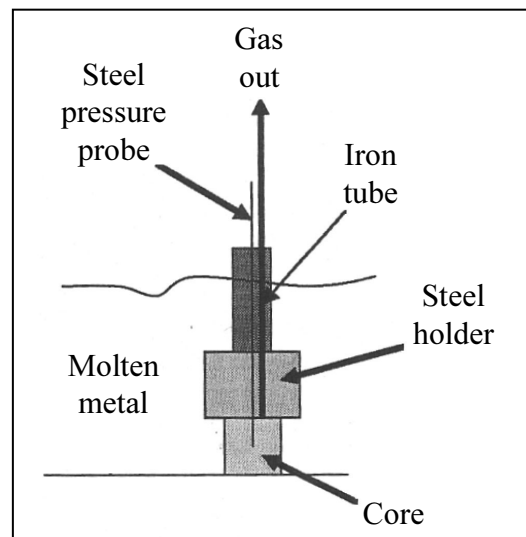


(b)

Figure 4: Experimental methods employed by Bates and Monroe [19] to measure the (a) volume and (b) pressure of gas evolved from bonded sand. The other sections of the castings' molds are not illustrated.



(a)



(b)

Figure 5: Techniques for measuring binder gas evolution from cores immersed in molten metal: (a) displacement apparatus developed by Scarber *et al.* [28] for measuring the evolved binder gas volume; (b) modification of displacement apparatus by Winardi *et al.* [29] for measurement of the binder gas pressure inside the test core.

CHAPTER 3. EXPERIMENTAL METHODS

3.1 Experimental Approach of Present Study

In the present study, the mass and molecular weight of the binder gas evolved during decomposition of PUNB bonded sand is measured under conditions similar to those experienced during casting. TGA is employed to measure the binder gas mass as a function of temperature for heating rates experienced in the mold and cores during casting processes. A specially designed quartz manometer is used to measure the binder gas volume, pressure, and temperature during heating and cooling in a furnace. These gas evolution measurements are combined with the ideal gas law to determine the binder gas molecular weight as a function of temperature. The bonded sand is immersed in an inert atmosphere during the experiments to ensure that the binder pyrolyzes, which is reflective of the binder decomposition behavior experienced during casting. Unlike in previous studies, the evolved binder gas is contained and measured entirely within the “hot zone” of a furnace, which eliminates the potential for undesired binder gas condensation during heating and other issues related to non-localized gas measurement. The present experimental techniques also allow for continuous measurement of the binder gas molecular weight variations with temperature.

3.2 Preparation of Specimens

The PUNB bonded sand specimen composition and preparation procedure follow those employed by Thole and Beckermann [32]. Specimens of bonded sand were prepared from IC55 silica lake sand, black iron oxide (BIO), and a PUNB binder system. The values for the binder content (1.25% of total mass), binder ratio (60:40 ratio of Part 1 to Part 2), catalyst percentage (8% of total binder mass), and additives (BIO, 3% of total mass) were selected based on feedback from seven steel foundries.

The sand and BIO components were measured using an Ohaus model PA4101 precision balance, and the binder components were measured using a Denver Instruments

model S-403 precision balance. The specimens were prepared by first mixing the BIO into the sand with a KitchenAid® standing mixer to ensure uniform particulate distribution. Then the binder was added according to a procedure recommended by the binder manufacturer. Part 1 (Pep Set® X1000) and Part 3 (Pep Set® 3500) were combined in a paper cup and subsequently added to the particulate mixture. The batch was mixed for 45 seconds, and then vigorously tossed to bring the coated mixture from the bottom of the mixing bowl to the top. The batch was mixed for another 45 seconds and tossed again. After the second toss, Part 2 (Pep Set® X2000) was added to the batch and mixed for another 45 seconds, which was followed by a third tossing. The batch was mixed for a final 45 seconds before dumping it into a box with rectangular patterns. The sand-binder mixture was rammed by hand into each pattern, while making sure the specimens were of uniform density, and allowed to set in the box before stripping (removal of the specimens from the pattern box). The bonded sand specimens were stripped when the compacted mixture withstood 20 psi of compressive stress without visible deformation [14]. The pattern box was capable of making six bonded sand blocks, each with a 2.54 cm (1 in) square cross-section and a 22.88 cm (9 in) length. The specimens were immediately sealed in plastic bags to minimize evaporation of the solvents, and the specimens were allowed to cure inside the bags for at least 24 hours prior to testing.

Small specimens of pure PUNB binder were prepared using the same binder system, binder ratio, and catalyst percentage as the bonded sand specimens. The pure binder specimens were prepared by first combining Part 1 and Part 3 in a paper cup. Then Part 2 was added to the other binder components, and the mixture was vigorously stirred for 10 seconds. The mixture was immediately poured into a small mold with rectangular patterns. Once the liquid binder mixture solidified, the pure binder specimens were removed from the pattern and immediately sealed in plastic bags. Like the bonded sand specimens, the pure binder specimens were allowed to cure inside the bags for at least 24 hours before testing.

3.3 Thermogravimetric Analysis

TGA was performed on PUNB bonded sand and pure PUNB binder using a PerkinElmer model Pyris 1 thermogravimetric analyzer. This machine measured the mass and temperature of a sample of interest during heating at a specified rate. The PUNB bonded sand specimens were cut down into smaller pieces, which were then shaped into small cylinders using a razor blade. The PUNB bonded sand samples for TGA were approximately 55 mg, and the samples were about 0.45 cm in diameter and 0.25 cm in height. The pure PUNB binder specimens were pulverized into small particles. The pure binder samples for TGA measured approximately 7.5 mg.

The TGA machine was purged with argon gas, and the total gas flow rates employed were 80 cm³/min (60 cm³/min to the balance and 20 cm³/min to the sheath) and 25 cm³/min (15 cm³/min to the balance and 10 cm³/min to the sheath). The 25 cm³/min total flow rate was specifically chosen in order to minimize nonisothermality in the samples during testing. The argon gas flow created a bias in the TGA machine's mass measurements, which necessitated separate measurement of the initial sample mass. The initial mass of each sample was measured using a Mettler-Toledo model AB135-S analytical balance prior to testing.

The samples were heated from room temperature to 1000°C at rates of 2°C/min, 10°C/min, and 100°C/min. The heating rates for TGA were selected to reflect those experienced in the mold during actual casting processes. The high heating rate of 100°C/min simulated mold and core heating rates at a distance of about 0.5 in from the mold-metal interface, and the 2°C/min and 10°C/min heating rates simulated mold and core heating rates at distances further away from the mold-metal interface. Multiple tests were performed at each heating rate to verify repeatability of the experiments. The TGA machine was allowed to self-clean periodically between tests, and the sample pans were cleaned according to the recommendations of the manufacturer.

The fraction of original binder mass remaining f in a PUNB bonded sand sample

or a pure PUNB binder sample as a function of temperature during heating was calculated by

$$f = 1 - \frac{m_s(T^0) - m_s(T)}{m_s^0 \chi / 100} \quad (1)$$

where m_s is the sample mass measured by the TGA machine at both the initial sample temperature T^0 and varying sample temperature T , m_s^0 is the initial sample mass measured with the analytical balance, and χ is the binder content of the samples based on the total weight percentage. The binder content for the pure binder samples was obviously 100%. The fraction of original binder mass remaining in bonded sand during heating was interpolated at intervals of 0.1°C from the corresponding fractions obtained from the TGA measurements. This allowed the measurements of the binder gas mass evolution to be matched with the measured binder gas volume and pressure (obtained from later gas evolution experiments) at discrete temperature points.

3.4 Gas Measurement Apparatus

A schematic of the apparatus developed in the present study to measure the volume, pressure, and temperature of gas during heating or cooling is shown in Figure 6. The primary component is the gas evolution device (GED), made by fusing quartz cylinders and discs together. Cylinder 1 of the GED was sealed at the top and bottom and had two quartz thermocouple wells attached to the top surface. One thermocouple well extended up from the top of cylinder 1, while the other extended 2 cm from the top surface down into the interior of cylinder 1. Cylinder 1 had an internal diameter of 4 cm and a height of 3 cm. Cylinder 2 of the GED was sealed at the bottom, had an internal diameter of 1.3 cm, and had a height of 22 cm. Cylinders 1 and 2 were joined by a third quartz tube, creating a container with a “J-shaped” cavity that acted as a manometer.

A sample of interest was loaded into cylinder 1 of the GED, and the GED was

filled with a eutectic alloy of gallium (75% by mass) and indium (25% by mass) to a specified initial height in cylinder 2. The metal alloy is liquid at room temperature and has low vapor pressures at high temperatures. Specific filling procedures will be described later. A displacement boat, which was a quartz tube with the bottom end sealed, was inserted into cylinder 2 such that the boat rested on top of the liquid metal. The displacement boat's outer diameter was 1.15 cm, which allowed for smooth vertical translation of the boat in cylinder 2. The boat's bottom surface was flat on the exterior and spherical on the interior.

The filled GED was placed on top of a square quartz plate, with 10 cm sides and 0.3 cm thickness, inside a Neytech model 85P radiative furnace capable of reaching 1100°C. Three specially made ceramic-insulated Type K thermocouples were used to measure the furnace temperature (the bead touched the interior of a protective quartz sheath), the glass temperature at the top surface of cylinder 1 (the bead touched the bottom of the glass well), and the interior temperature of the liquid metal in cylinder 1 (the bead touched the bottom of the metal well). A displacement probe was threaded through a small hole in a stabilizer plate (attached to the top of the furnace) and then lowered down to rest on the interior spherical surface of the displacement boat. The displacement probe was a thin quartz rod attached to a thin 2.5 cm square quartz plate that was covered with black spray paint on the top surface. Argon was supplied to cylinder 2 at a rate of 200 cm³/min in order to prevent the liquid metal from oxidizing during the experiments.

A Micro-Epsilon model optoNCDT 1400 laser optical displacement sensor was mounted to a support rig above the furnace, powered by a Topward model 3306D power supply, and carefully calibrated to measure the vertical position of the displacement probe's square plate. A square steel tube was placed around the probe to reduce displacement measurement noise caused by disturbances from the surroundings. A fan forced air over the furnace to keep the laser sensor cool during tests, and the temperature

near the laser sensor was monitored with a fourth Type K thermocouple.

The experimental data was collected using an IOtech model 3005 Personal DAQ system connected to a laptop via USB. DASyLab[®] software [33] was used to control the data acquisition system. Sampling was performed at a frequency of 10 Hz for all measurements, and this raw data was averaged and recorded at a frequency of 2 Hz.

In a typical experiment, the initial height of the probe was measured by the laser sensor for 5 minutes prior to the start of the test. The furnace was heated at a constant rate and the contents of the GED expanded. This caused the metal height in cylinder 2 to rise. The metal displacement moved the position of the displacement probe, and the probe's vertical translation was detected by the laser sensor. Thus, the total expansion of the GED's contents was measured as a function of temperature. Tests were monitored to ensure that the liquid metal did not overflow in cylinder 2. Cooling data were collected for some tests, and cooling was performed by turning the furnace off and allowing the GED to naturally cool to room temperature. After testing, the GED was removed from the furnace and the GED's contents were emptied. The liquid metal and GED were cleaned using a solution of low molarity hydrochloric acid, and any remaining particulate matter was removed from the liquid metal. The GED was then washed with acetone, dried, and heated in the furnace to volatilize any residual organic matter.

3.5 Metal-Only Expansion Tests

It was necessary to determine the expansion behavior of the liquid metal as a function of temperature. This was achieved by measuring the metal expansion in the GED during heating.

The filling process for the metal-only expansion tests is illustrated in Figure 7 (a-f). The empty GED was rotated to induce a slight incline and clamped to a lab stand as shown in Figure 7 (a). Two flexible plastic tubes were fed through a long and narrow glass tube with a rubber stopper attached at one end. One plastic tube was connected to

an argon gas supply, and the other plastic tube was connected to a syringe filled with liquid metal. The glass tube with the stopper, hereafter referred to as the filling fixture, acted as a barrier between the plastic tubes and the internal surface of cylinder 2 of the GED. Any excess metal that adhered to the inside of cylinder 2 interfered with the mass measurements of the filled GED and the ability of the displacement boat to translate in a smooth vertical manner. Use of the filling fixture ensured that the internal surface of cylinder 2 remained clean during filling. Inserting the tubes through the filling fixture also provided better control of the position of the tubes within the GED. The outlets of the argon and metal injection tubes were placed inside cylinder 1 near the opening of the GED's connecting tube. The GED was purged with argon at a rate of $400 \text{ cm}^3/\text{min}$ for 10 minutes prior to filling, and this flow rate was maintained throughout the filling process. The GED in the pre-filled state can be seen in Figure 7 (b). Liquid metal was injected into cylinder 1 of the GED, shown in Figure 7 (c), and the filling continued until the GED's connection tube was closed off by liquid metal as illustrated in Figure 7 (d). The GED was rotated back to an upright position, and a third plastic tube attached to a pipette filler bulb was fed through the filling fixture. The outlet of the third tube was positioned near the top corner of cylinder 1 as seen in Figure 7 (e). The remainder of cylinder 1 was filled with liquid metal by evacuating cylinder 1 with the pipette bulb while simultaneously injecting additional metal into cylinder 2. After cylinder 1 was completely filled, the evacuation tube was removed and additional liquid metal was injected into the GED such that the initial metal height in cylinder 2 (h_2^0) was 3.5 cm. This height was selected to ensure that the metal level in cylinder 2 was initially higher than the metal level in cylinder 1 (creating positive pressure in cylinder 1). The GED in the filled state for the metal-only tests is shown in Figure 7 (f).

The mass of the empty and filled GED was measured for all experiments using an Ohaus model EP613C precision balance. The metal mass was found by simply subtracting the metal-filled GED mass from the empty GED mass. Once the GED was

filled and the mass measurements were obtained, the displacement boat was lowered onto the metal surface in cylinder 2 and the GED was placed in the furnace. Then the thermocouples were positioned in their proper locations and the initial height of the displacement probe was measured by the laser sensor. The initial metal heights in cylinders 1 and 2 were measured with a precision ruler. The furnace was heated at a constant rate ranging between 2°C/min and 15°C/min while temperature and expansion measurements were obtained. Multiple tests were performed to ensure that the experiments were repeatable. The density of the liquid metal at room temperature (i.e., the initial temperature) was obtained by measuring the mass of metal that filled a calibrated volumetric flask. The metal density at room temperature was measured prior to filling the GED for all experiments.

The effective volumetric expansion coefficient of the liquid metal in the GED β_m^{eff} as a function of temperature was calculated from the metal-only expansion measurements and found by

$$\beta_m^{eff} = \frac{\frac{\pi}{4} D_2^2 \Delta h_2}{(T_m - T_m^0)} \left(\frac{\rho_m^0}{m_m} \right) \quad (2)$$

where D_2 is the internal diameter of cylinder 2 of the GED, Δh_2 is the measured height change in cylinder 2, T_m is the measured metal temperature, T_m^0 is the measured initial metal temperature, ρ_m^0 is the density of the liquid metal at room temperature, and m_m is the mass of liquid metal in the GED.

Additional experiments were carried out to determine the true volumetric expansion coefficient of the liquid metal. A spherical borosilicate bulb was fused to a long and narrow borosilicate tube. The bulb was filled with liquid metal, placed in the furnace, and subjected to a step-heating program that simulated an “infinitely slow” heating rate. A second volumetric expansion coefficient was calculated using the measurements from the metal-only expansion in the bulb and Equation 2 (with D_2

replaced by the bulb tube's inner diameter and Δh_2 replaced by the metal-only height change measured in the bulb tube).

3.6 Pure Gas Expansion Tests

A range of volumes of argon and hydrogen gases and the liquid metal were heated in the GED. This was done to observe the behavior of gas expansion in the GED and to determine the accuracy to which the gas measurement apparatus could measure the molecular weight of a known gas.

The filling process for the pure gas expansion tests is illustrated in Figure 8 (a-d). The GED was first filled entirely with liquid metal following the metal-only procedure illustrated in Figure 7 (a-f), and Figure 8 (a) shows the state of the GED prior to insertion of the gas sample. The metal injection tube was repositioned and argon gas flowed into cylinder 2 of the GED as shown in Figure 8 (b). The argon gas flowed into cylinder 2 at a rate of 400 cm³/min. A third plastic tube attached to a syringe containing the gas sample was fed through the filling fixture. The outlet of the third tube was positioned near the top corner of cylinder 1. The gas sample was injected into cylinder 1 while liquid metal was simultaneously removed from cylinder 2, as shown in Figure 8 (c). This continued until the entire gas sample was inside cylinder 1 of the GED. The gas injection tube was removed from the GED, and the liquid metal level was adjusted such that the initial metal height in cylinder 2 was 3.5 cm. The GED in the filled state for the pure gas expansion tests is shown in Figure 8 (d).

After the GED was filled, the remainder of the test preparation was completed as previously described. The furnace was heated at a rate of 2°C/min, 3°C/min, and 10°C/min while temperature and expansion measurements were obtained. Multiple pure argon and pure hydrogen expansion tests employing various initial sample volumes were performed to confirm repeatability of the experiments.

The gas temperature T and initial temperature T^0 were not directly measured.

Instead, these temperatures were assumed to be equivalent to the measured metal temperature and measured initial metal temperature, respectively. The reasoning behind this will be discussed later. The measured metal height change in cylinder 2 during heating of the gas samples was used to interpolate the corresponding height change at intervals of 0.1°C over the measured temperature range. This was done to properly match the pure gas measurements with the metal expansion data, as well as to standardize the pure gas expansion measurements and subsequent calculations as a function of temperature.

The total gas volume V_g as a function of temperature was found as

$$V_g = \left(V_{fill}^0 - \frac{m_m}{\rho_m^0} \right) + \left(\frac{\pi D_2^2}{4} \Delta h_2 - \Delta V_m \right) \quad (3)$$

where V_{fill}^0 is the volume contained by the filled GED (up to h_2^0) at the initial temperature and ΔV_m is the change in volume of the liquid metal. The first term in Equation 3 corresponds to the initial gas volume V_g^0 (which was verified against the supposed volume of gas injected into the GED), and the second term in Equation 3 corresponds to the change in gas volume ΔV_g as a function of temperature. The volume change of the liquid metal in the GED corresponding to a given temperature change was derived as [34]

$$\Delta V_m = \beta_m^{eff} \left(\frac{m_m}{\rho_m^0} \right) (T - T^0) \quad (4)$$

As previously stated, the GED acted as a manometer, and the total gas pressure P_g as a function of temperature was found by [35]

$$P_g = \rho_m g \Delta H + P_{atm} + P_{probe} \quad (5)$$

where ρ_m is the density of the liquid metal at a given temperature, g is gravitational

acceleration (9.81 m/s^2), ΔH is the height difference between the metal surfaces in cylinders 1 and 2, P_{atm} is atmospheric pressure (101325 Pa), and P_{probe} is the pressure from the weight of the displacement probe and boat. The density of the liquid metal at a given temperature was described by

$$\rho_m = \frac{\rho_m^0}{1 + \beta_m^{eff} (T - T^0)} \quad (6)$$

The height difference between the metal surfaces in cylinder 1 and 2 was straightforwardly calculated as

$$\Delta H = (h_2^0 - h_1^0) + (\Delta h_2 + \Delta h_1) \quad (7)$$

where h_1^0 is the initial metal height in cylinder 1, and Δh_1 is the metal height change in cylinder 1. The metal height change in cylinder 1 of the GED was found as

$$\Delta h_1 = \frac{4 \Delta V_g}{\pi D_{1,eff}^2} \quad (8)$$

where $D_{1,eff}$ is the effective internal diameter of cylinder 1.

The molecular weight of an ideal gas M_g (being a single gas or a gas mixture) can be derived from the ideal gas law defined as [36]

$$M_g = \frac{m_g \bar{R} T}{P_g V_g} \quad (9)$$

where m_g is the total gas mass and \bar{R} is the universal gas constant (8.314 J/mol/K). Manipulation of Equation 9 produces the ratio of the measured to known molecular weight (or simply the dimensionless molecular weight) φ of a single gas i such that

$$\phi = \frac{M_g}{M_i} = \left(\frac{P_g^0}{P_g} \right) \left(\frac{V_g^0}{V_g} \right) \left(\frac{T}{T^0} \right) \quad (10)$$

where M_i is the true molecular weight of the measured gas i and P_g^0 is the initial gas pressure found by inputting the initial measurement conditions into Equation 5. The accuracy to which the apparatus could measure the molecular weight of a known gas was evaluated through the dimensionless molecular weight measurements.

3.7 Binder Gas Evolution Tests

PUNB bonded sand samples for gas evolution measurement were prepared using the same methods as those used for TGA. The bonded sand samples for gas expansion measurement were shaped into small cylinders measuring about 0.8 cm in diameter and 0.5 cm in height, and the mass of the samples was approximately 0.2 g. The sample mass was measured with the same device used to measure the empty and filled GED. The small sample size minimized nonisothermality in the samples during testing, and multiple samples were used in each experiment to achieve the desired total initial sample mass.

It is important to note that the PUNB bonded sand samples had a porosity of about 33% [32]. The presence of even small amounts of air in the samples would create non-ideal conditions for bonded sand pyrolysis, which needed to be avoided. Therefore, the bonded sand samples were placed in a plastic bag that was continuously flushed with argon gas for 15 minutes. The samples were stored in the argon-filled plastic bag for at least 24 hours prior to testing. These methods were employed to ensure that only argon occupied the empty space inside the samples when they were loaded into the GED.

The filling process for the binder gas evolution tests is illustrated in Figure 9 (a-f). The GED was first filled according to the steps outlined in Figure 7 (a-c), and Figure 9 (a) shows the state of the GED prior to insertion of a bonded sand sample. The filling fixture and the argon gas and liquid metal injection tubes were removed from the GED. A bonded sand sample was placed inside a small cup attached to a long and narrow rod, and

the sample was lowered into cylinder 2 of the GED as shown in Figure 9 (b). Loading samples using the cup and rod assembly standardized the sample insertion process. The sample slid into cylinder 1 and rested against the liquid metal, and the cup and rod assembly was removed from the GED. It was desirable to have the samples float on top of the liquid metal during filling. The argon injection tube was fed into cylinder 1 of the GED, and a burst of argon gas pushed the sample on top of the liquid metal as illustrated in Figure 9 (c). The steps outlined in Figure 9 (b-c) were repeated until all samples for a given test were loaded in the GED. The loaded samples were then purged with argon gas at a flow rate of 400 cm³/min for 10 minutes to remove any air that the samples may have picked up during the loading process. The remainder of the filling process is shown in Figure 9 (d-f), which follows the corresponding steps for the metal-only filling procedure previously described.

After the GED was filled, the remainder of the test preparation was completed as previously described. The metal mass in the GED was found by subtracting the total filled mass of the GED from the total mass of the samples in the GED. The furnace was heated at a rate of 2°C/min while temperature and expansion measurements were obtained. The heating rate was selected based on the results from the pure gas expansion tests. Multiple experiments were performed to obtain the binder gas molecular weight for all temperatures of interest. Total initial sample masses ranged from about 0.4 g to 9 g, with larger sample masses corresponding to tests performed to lower maximum temperatures. In addition, measurements were collected as the furnace cooled during some of the tests.

The temperatures of the bonded sand samples, argon gas inside the bonded sand samples, and evolved binder gas in the GED were not directly measured. These temperatures were assumed to be equivalent to the measured metal temperature. The validity of this assumption will be addressed later in the discussion.

It is important to note that the TGA machine directly measured the temperature of

the bonded sand during heating (not the temperature of the evolved gas), whereas the bonded sand and evolved binder gas are assumed to be at the same temperature during heating in the GED. A common assumption employed in binder gas modeling is that the evolved binder gas temperature is equivalent to the local temperature of the bonded sand mold or core [10-12]. Therefore, it was reasonable to assume that the temperature of the binder gas evolved during TGA of bonded sand samples was equivalent to the bonded sand sample temperature measured by the TGA machine. By simple conservation of mass, the binder mass lost during heating is equivalent to the binder gas mass evolution. Thus, the mass of binder gas evolved from the bonded sand m_b as a function of temperature was found by

$$m_b = (1 - f) \left(m_s^0 \frac{\chi}{100} \right) \quad (11)$$

where m_s^0 is the total initial PUNB bonded sand sample mass placed in the GED.

A mixture of argon and binder gas was present during heating of the PUNB bonded sand samples. Interpolations of the measured metal height change in cylinder 2 were performed such that the total gas volume and pressure could be determined at intervals of 0.1°C over the measured temperature range. The total gas volume and pressure were found using the same methods as described for the pure gas volume and pressure calculations. Equation 9 may only be used to calculate the effective molecular weight of the argon and binder gas mixture as a function of temperature. The molecular weight of the evolved binder gas M_b as a function of temperature was derived through summation of the partial pressures of the argon and binder gases along with manipulation of Equation 9 such that

$$M_b = \frac{m_b \bar{R}}{\left(\frac{P_g V_g}{T} - \frac{P_g^0 V_g^0}{T^0} \right)} \quad (12)$$

The interpolation of the binder gas mass evolution, volume, and pressure measurements at intervals of 0.1°C allowed the data sets to be matched together when the experiments employed the same heating rate. This enabled Equation 11 to be directly inserted into Equation 12, and the binder gas molecular weight as a function of temperature was straightforwardly calculated.

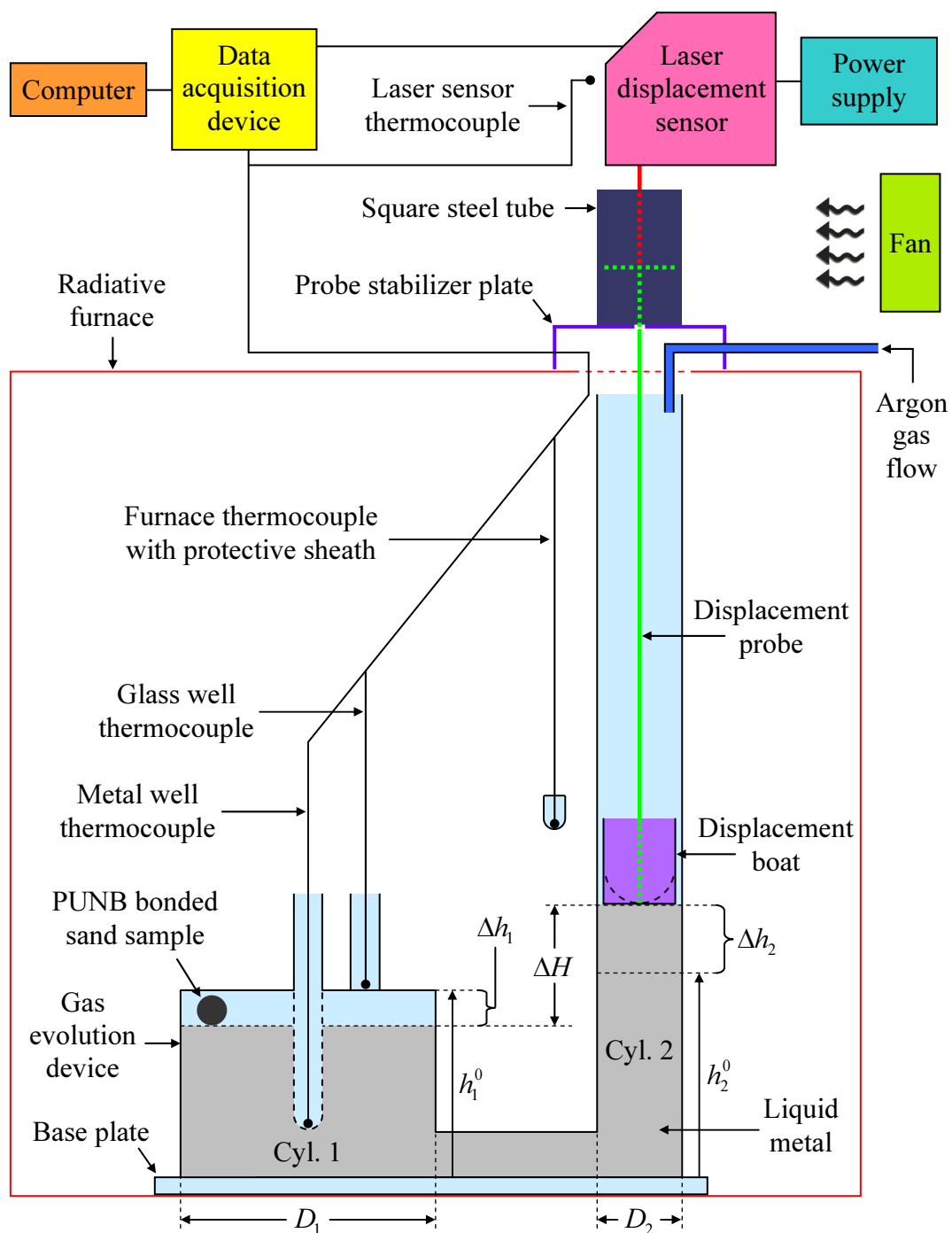


Figure 6: Schematic of gas measurement apparatus and important geometric quantities.

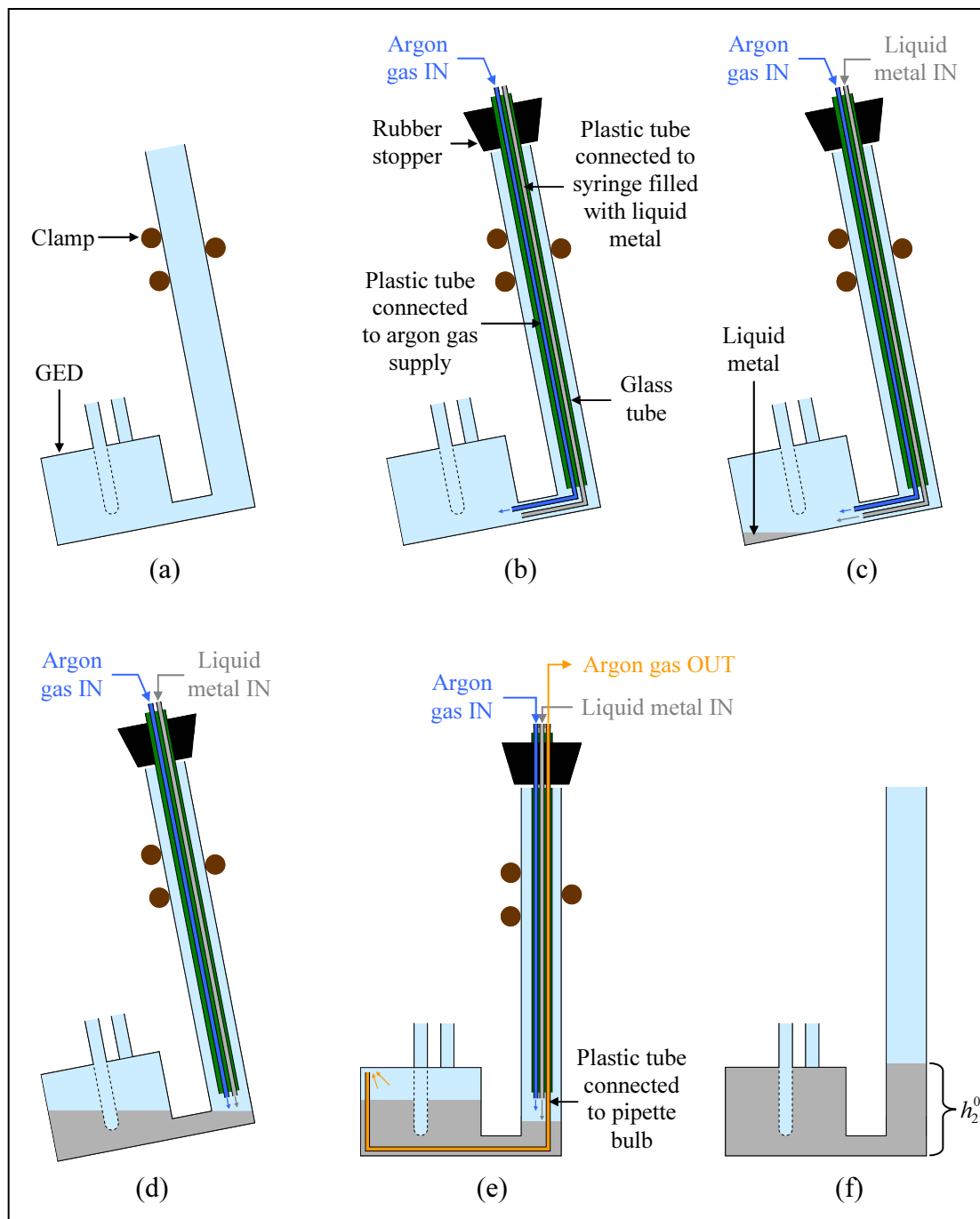


Figure 7: Procedure for filling GED with only liquid metal: (a) rotate and clamp GED to lab stand; (b) insert argon and liquid metal injection tubes into filling fixture and place fixture in cylinder 2, purge GED with argon; (c) begin filling GED with liquid metal; (d) continue to fill GED with liquid metal until the connection tube of the GED is closed off by liquid metal; (e) insert argon evacuation tube through filling fixture and into cylinder 1, evacuate argon in cylinder 1 while injecting argon and additional liquid metal into cylinder 2 until cylinder 1 is filled with liquid metal; (f) fill cylinder 2 with liquid metal such that $h_2^0 = 3.5$ cm.

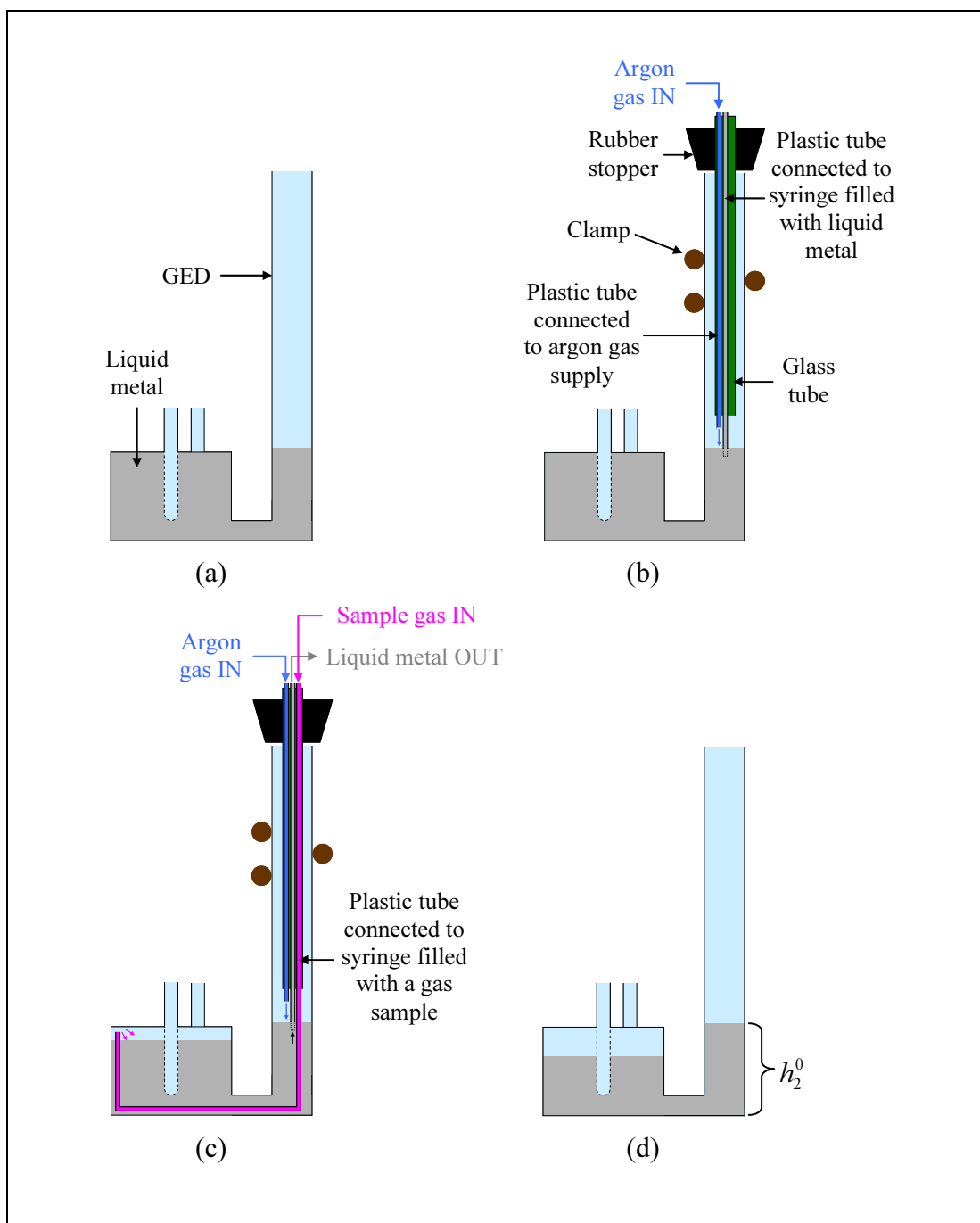


Figure 8: Procedure for filling GED with a gas sample and liquid metal: (a) continued from Figure 7 (f); (b) insert argon and liquid metal injection tubes into filling fixture and place fixture in cylinder 2, purge cylinder 2 with argon; (c) insert gas sample injection tube through filling fixture and into cylinder 1, inject gas sample into cylinder 1 while simultaneously extracting liquid metal from cylinder 2, continue to inject the gas sample and extract liquid metal until the entire gas sample is in cylinder 1; (d) fill cylinder 2 with liquid metal up to the set initial height h_2^0 of 3.5 cm.

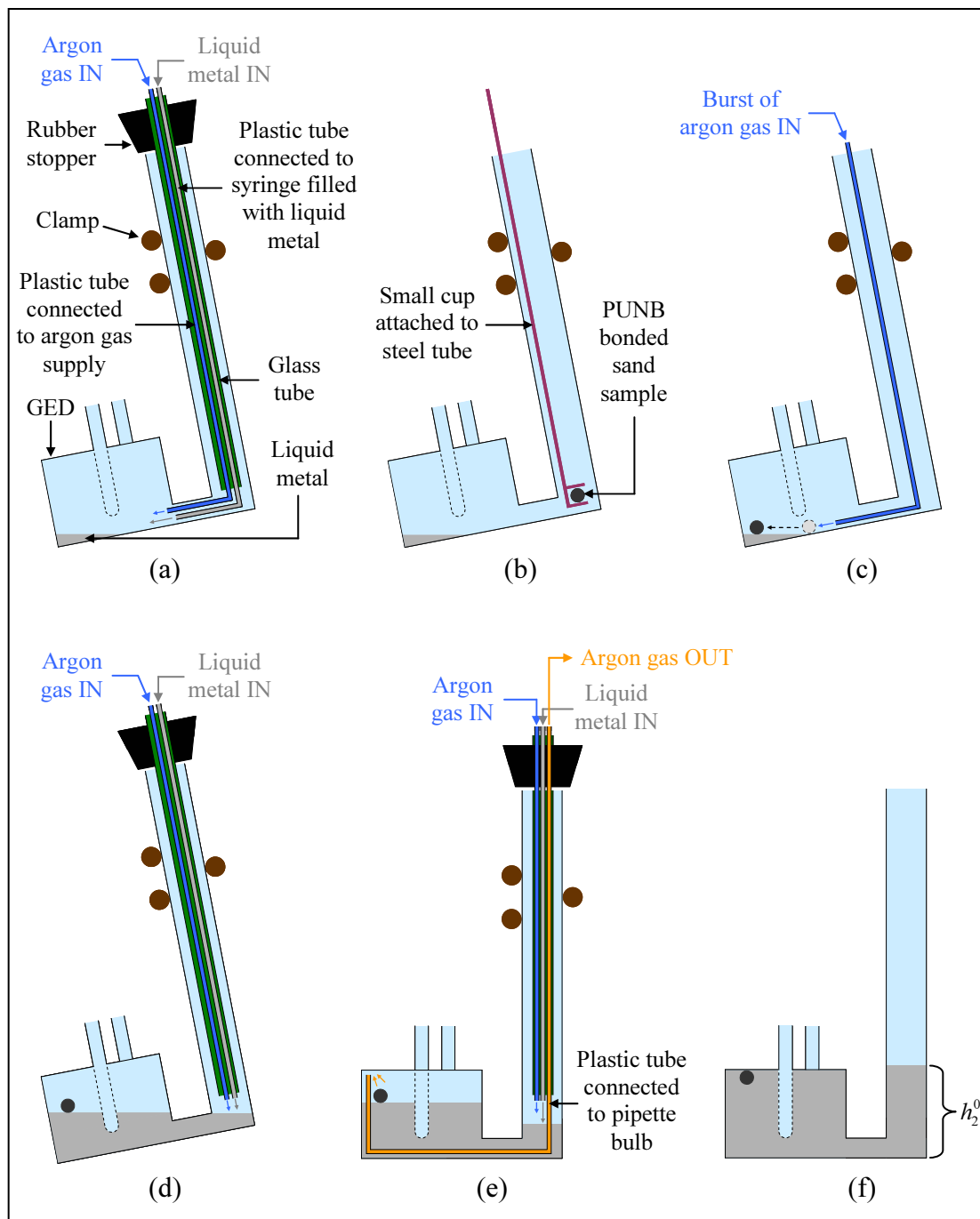


Figure 9: Procedure for filling GED with a PUNB bonded sand sample and liquid metal: (a) continued from Figure 7 (c); (b) remove filling fixture and lower PUNB bonded sand sample into cylinder 2 with cup and rod assembly; (c) use argon gas flow to position the bonded sand sample on top of liquid metal; (d) continue to fill GED with liquid metal until the connection tube of the GED is closed off by liquid metal; (e) insert argon evacuation tube through filling fixture and into cylinder 1, evacuate argon in cylinder 1 while injecting argon and additional liquid metal into cylinder 2 until cylinder 1 is filled with liquid metal; (f) fill cylinder 2 with metal up to the set initial height h_2^0 of 3.5 cm.

CHAPTER 4. RESULTS AND DISCUSSION

4.1 Thermogravimetric Analysis

The following sub-sections describe the results from preliminary TGA as well as from TGA for PUNB bonded sand and pure PUNB binder.

4.1.1 Preliminary TGA Measurements

Preliminary experiments were performed to compare the decomposition behavior of 55 mg samples of PUNB bonded sand and pure IC55 silica sand for a heating rate of 100°C/min with a total argon gas flow of 80 cm³/min. TGA of the pure sand was of interest because the sand comprises the majority of the bonded sand mass, and it was important to determine whether sand decomposition significantly contributes to gas evolution. Measurements of the bonded sand and pure sand mass change representative of the preliminary test results are illustrated in Figure 10. It can be seen that the PUNB bonded sand loses far more mass (thereby evolving more gas) than the pure sand during heating. This is expected, and the mass loss in the pure sand is likely due to trace impurities being volatilized. In addition, Figure 10 shows that the bonded sand and pure sand mass change increases at the same rate from 20°C to 115°C. The abnormal increase in the measured sample mass required additional investigation.

The TGA machine's empty sample pan was heated from room temperature to 1000°C at a rate of 100°C/min with 80 cm³/min of argon flow, and the empty sample pan mass change results are superimposed on those of the bonded sand and pure sand in Figure 10. There should be no change in the empty sample pan mass, but this is clearly not the case. Rather, the measured mass change varies with temperature. What is most interesting is that the small increase in the empty sample pan mass at very low temperatures coincides with portions of both the bonded sand and pure sand curves. It was hypothesized that the TGA machine's mass measurements contained a temperature-related bias and that the presence of the samples affected the bias. In light of this, TGA

was performed on 61 mg of broken quartz rods from room temperature to 1000°C at a heating rate of 100°C with 80 cm³/min of argon flow. The quartz rod mass should not change within this temperature range, and the quartz rod mass was chosen to mimic the bonded sand and pure sand sample masses. The measured mass change of the quartz rods is illustrated with the other mass change curves in Figure 10. Like the empty sample pan measurements, the quartz rod mass change varies with temperature. Unlike the empty sample pan measurements, however, the increase in the measured quartz rod mass from 20°C to 115°C directly coincides with the increase in the measured bonded sand and pure sand sample masses. Additional quartz rod tests for a heating rate of 100°C/min showed that the variations in the measured mass change were reproducible. Temperature-dependent variations in quartz rod mass measurements were also obtained at heating rates of 2°C/min and 10°C/min. This proved that the increase in the measured mass of the bonded sand and pure sand samples was entirely due to a bias in the TGA machine's mass measurements. These variations were found to be unaffected by the argon flow rate. The mass change measurements from TGA of the quartz rod samples for heating rates of 2°C/min, 10°C/min, and 100°C/min are shown in Figure 11. It can be seen that the measured mass change at heating rates of 2°C/min and 10°C/min are essentially identical, and the high heating rate of 100°C/min induces a different behavior in the mass reading bias.

The quartz rod data was used to account for the temperature-dependent bias in the TGA machine's mass measurements and correct the TGA mass measurements for all other samples tested. The corrected and uncorrected percentage of mass remaining in a 55 mg PUNB bonded sand sample and a 7.5 mg pure PUNB binder sample during heating at a rate of 100°C/min with a total argon gas flow of 80 cm³/min is illustrated in Figure 12 (a-b). It can be seen that the artificial increase in the bonded sand sample mass is completely removed when the correction is applied. The bonded sand sample mass remains constant until binder decomposition begins, which is the expected behavior. The

correction also shifts the bonded sand mass curve down, which is reflective of the temperature-dependent erroneous increase in the measured mass being removed from the results. The pure binder mass curve is relatively unaffected by the TGA correction. This is because the pure binder loses a significant portion of its mass during heating, and the mass correction is small compared to the overall pure binder mass loss. All TGA results presented hereafter are corrected to account for the mass reading bias.

The relative mass loss in the bonded sand components as a function of temperature was of interest. Figure 13 compares the mass loss percentage in pure PUNB binder, pure sand, and pure BIO samples heated at a rate of 100°C/min with a total argon gas flow of 80 cm³/min. Again, the sand loses very little mass during heating. The BIO also experiences minor mass loss. As expected, the PUNB binder loses far more mass during heating than its sand and BIO counterparts. These results indicate that more than 91% of the mass loss in PUNB bonded sand during heating is due to decomposition of the binder. Therefore, to simplify the decomposition analysis, it was assumed that the measured mass loss in the bonded sand samples was entirely due to binder mass loss.

The effects PUNB bonded sand sample size on the binder decomposition was studied. The fraction of original binder mass remaining in 55 mg, 80 mg, and 100 mg PUNB bonded sand samples heated at a rate of 100°C/min with a total argon gas flow of 80 cm³/min is shown in Figure 14. It can be seen that increasing the sample mass from 55 mg to 80 mg or 100 mg does not affect the binder decomposition. Lowering the bonded sand sample mass below 55 mg was not desirable. This is because smaller samples were more likely to have non-homogeneous distribution of the binder within the sand and BIO, and non-homogenous binder distribution in the samples would be nonrepresentative of bonded sand used in casting processes.

4.1.2 Bonded Sand Decomposition Measurements

The fraction of original binder mass remaining in 55 mg PUNB bonded sand

samples heated at rates of 2°C/min, 10°C/min, and 100°C/min with total argon gas flow rates of 80 cm³/min and 25 cm³/min is plotted as a function of temperature in Figure 15 (a-b). Thanks to the correction of the TGA machine's mass measurements, the fraction of original binder mass curves with either flow rate remain at approximately 1 until binder decomposition begins. The curves are almost horizontal when the decomposition reaction is finished, indicating nearly complete removal of the TGA machine's mass measurement bias. It should be noted that applying the correction changes the bonded sand fraction of original binder mass by as much as 10% at the maximum decomposition temperature. There is good repeatability in the bonded sand fraction of original binder mass remaining for each heating rate specific to each flow rate. It can be seen from Figure 15 (a-b) that there is an increasing delay in the start of decomposition with increasing heating rate. Decomposition reactions are kinetic in nature, meaning that the decomposition depends on the absolute temperature and the time spent at that temperature. Subsequently, an increase in the sample heating rate shifts the onset of decomposition to higher temperatures. Overall, however, the decomposition behavior is similar between heating rates.

The differences in the fraction of original binder mass remaining in bonded sand between corresponding heating rates at each flow rate are less than 5% from 20°C to 540°C. It is quite clear from Figure 15 (a-b), however, that both the fraction of original binder mass remaining as a function of temperature above 540°C and the completion of the binder gas decomposition are affected by the gas flow rate. The fraction of original binder mass remaining in bonded sand corresponding to 80 cm³/min of gas flow decreases in an essentially linear manner with temperature, and the samples at this flow rate corresponding to the 2°C/min heating rate achieve completion of the binder decomposition by about 865°C. The decrease in the fraction of original binder mass remaining in bonded sand for 25 cm³/min of gas flow is a more complex function of temperature. The bonded sand decomposition with 25 cm³/min of gas flow is complete by

about 700°C during heating at a rate of 2°C/min and at 800°C during heating at rates of 10°C/min and 100°C/min.

It is hypothesized that the bonded sand samples were less isothermal when a higher flow rate was utilized. This makes sense in that a greater amount of relatively cold gas entered the furnace area when a higher flow rate was used, which decreased the heat transfer to the samples. The gas also impinged on the top of the samples at a higher velocity for higher flow rates, thereby increasing the heat transfer away from the top of the samples and further promoting sample nonisothermality. Sample nonisothermality will not only change the decomposition reaction kinetics but also detrimentally affect the measurement of the sample temperature. Thus, it is concluded that the bonded sand decomposition as a function of temperature was more accurately measured when the total argon gas flow rate through the TGA machine was 25 cm³/min.

The TGA and gas measurement tests need to be performed at the same heating rate in order to properly measure the binder gas molecular weight as a function of temperature. As previously indicated, the variation in the bonded sand decomposition behavior (equivalent to the binder gas mass evolution behavior) is similar between heating rates. Therefore, it is speculated that the molecular weight of gas evolved from PUNB bonded sand should be roughly the same for heating rates of 2°C/min, 10°C/min, and 100°C/min. It was later found that the heating rate of the GED needed to be low to facilitate accurate measurement of the binder gas molecular weight, and the explanation for this will be given later in the discussion. Consequently, the measurements of the fraction of original binder mass remaining in the bonded sand samples heated at a rate of 2°C/min with 25 cm³/min of argon gas flow were fit to a set of piecewise polynomials for use in the binder gas molecular weight calculations. Additional modifications were made such that the fitted fraction of original binder mass remaining was set to 1 below 50°C and 0.1807 (the minimum fraction of original binder mass in bonded sand for a heating rate of 2°C/min) above 710°C. The polynomial fit of the fraction of original binder mass

remaining is superimposed on the corresponding measurements in Figure 15 (b), and the equations of these polynomials are listed in Table 4.

The measurements of the fraction of original binder mass remaining in bonded sand samples from the present study were averaged and compared against the results from previous studies as seen in Figure 16 (a-b). Lytle [23] performed TGA on 1.5% PUCB bonded sand (45:55 ratio of Part 1 to Part 2) at a heating rate of 150°C/min with 100 cm³/min of total nitrogen gas flow. Wang *et al.* [24] performed TGA on 1.5% PUCB bonded sand (45:55 ratio of Part 1 to Part 2) at a heating rate of 10°C/min under an argon atmosphere. Figure 16 (a) shows that the present bonded sand decomposition measurements for a gas flow rate of 80 cm³/min are in fairly good agreement with the results from References [23] and [24]. It is also interesting to note from Figure 16 (b) that the general behavior of the bonded sand decomposition from the present measurements with 25 cm³/min of gas flow is similar to that from Reference [23]. It is quite clear from Figure 16 (a-b) that care must be taken when comparisons are made between TGA measurements of bonded sand employing different purge gas flow rates.

4.1.3 Pure Binder Decomposition Measurements

Additional study of the decomposition of pure PUNB binder as a function of temperature was performed. Figure 17 (a-b) illustrates the fraction of original binder mass remaining in 7.5 mg pure PUNB binder samples (60:40 ratio of Part 1 to Part 2) heated at rates of 2°C/min, 10°C/min, and 100°C/min with total argon gas flow rates of 80 cm³/min and 25 cm³/min plotted as a function of temperature. Good repeatability is achieved at each heating rate specific to each gas flow rate. Like the bonded sand results, the heating rate seems to only significantly affect the onset of pure binder decomposition, and the decomposition behavior of the pure binder is affected by the gas flow rate. The differences in the fraction of original binder mass remaining in the pure binder between corresponding heating rates at each flow rate are less than 10% for all temperatures

studied. In addition, there is good agreement in the fraction of original binder mass remaining at the maximum decomposition temperature regardless of gas flow rate.

The measurements of the fraction of original binder mass remaining in pure PUNB binder samples from the present study were averaged and compared against the results from a previous study as seen in Figure 18 (a-b). Lytle [23] performed TGA on pure PUCB binder (45:55 ratio of Part 1 to Part 2) at a heating rate of 150°C/min with 100 cm³/min of total nitrogen gas flow. It can be seen that the present measurements at either flow rate agree reasonably well with the results from Reference [23] between 20°C and 150°C as well as between 500°C to 1000°C. The differences in the gas flow rates and sample heating rates employed in the present experiments and those of Reference [23] are the most likely causes of the discrepancies between the TGA results.

4.1.4 Comparison of Bonded Sand and Pure Binder

Decomposition Measurements

The average fraction of original binder mass remaining in PUNB bonded sand and pure PUNB binder samples at each heating rate and flow rate studied are shown in Figure 19. It is interesting that the variation in the pure binder decomposition behavior with 80 cm³/min of gas flow is similar to the bonded sand decomposition behavior with 25 cm³/min of gas flow. There is fairly good agreement in the fraction of original binder mass remaining at the maximum decomposition temperature for the bonded sand and pure binder with 80 cm³/min of gas flow.

For the most part, however, the general decomposition behaviors of the bonded sand and pure binder samples are dissimilar. The mass and physical condition of a given sample likely affects the heating of the sample, which will influence the decomposition reaction kinetics. The mass of the bonded sand samples was seven times greater than the mass of the pure binder samples. Furthermore, the bonded sand samples were whole pieces, as opposed to pulverized particulate matter like the pure binder samples, and the

bonded sand samples contained substantial amounts of solid particulate matter in addition to the binder. These factors are the most likely causes for the discrepancies between the bonded sand and pure binder decomposition behaviors at a given gas flow rate.

4.2 Metal-Only Expansion Measurements during Heating

Figure 20 shows the measured metal-only expansion in the GED during heating at constant rates ranging between 2°C/min and 15°C/min. The average heating rate of the liquid metal for the entirety of each experiment was always within $\pm 0.4^\circ\text{C}/\text{min}$ of the target heating rate, which was deemed acceptable. There is excellent repeatability in the height change measurements regardless of heating rate. It can be seen that the expansion behavior of the liquid metal changes at 200°C. The difference in the slope of the measured height change above and below 200°C is attributed to nonisothermality of the GED.

The effective volumetric expansion coefficient of the liquid metal was calculated as a function of temperature from the metal expansion measurements shown in Figure 20. The effective volumetric expansion coefficient describes the metal expansion behavior specific to the GED, and this coefficient is plotted in Figure 21. The volumetric expansion coefficients of the liquid metal calculated using the metal expansion measurements in the borosilicate bulb are essentially independent of temperature, and these coefficients are also shown in Figure 21. The coefficients obtained from the borosilicate bulb tests were averaged to determine a single temperature-independent volumetric expansion coefficient for the liquid metal. The constant volumetric expansion coefficient of the liquid metal β_m^{con} was found to be $1.12 \times 10^{-4} \text{ } 1/^\circ\text{C}$ and is superimposed on the other expansion coefficients illustrated in Figure 21.

The liquid metal's volumetric expansion and corresponding height change in the GED were predicted using β_m^{eff} and β_m^{con} , and the predicted metal height change is superimposed on the metal expansion measurements in Figure 22. The height change

predicted using β_m^{eff} coincides with the measured metal expansion because β_m^{eff} was derived directly from the metal height change measurements. It can be seen that curves corresponding to the measured metal expansion and the height change predicted using β_m^{con} are parallel above 200°C, implying that β_m^{con} is indeed the true volumetric expansion coefficient of the liquid metal. However, the actual expansion behavior of the liquid metal, inclusive of the nonisothermal effects below 200°C, is directly described by β_m^{eff} . Subsequently, β_m^{eff} was interpolated at intervals of 0.1°C from the corresponding values calculated from the metal-only expansion measurements in the GED. This allowed the metal expansion data to be properly applied to the pure gas expansion and binder gas evolution calculations. The average density of the liquid metal at room temperature was found to be 6.297 g/cm³.

4.3 Pure Gas Expansion Measurements during Heating

Figure 23 illustrates the measured total height change from expansion of the liquid metal and different initial volumes of pure argon gas and pure hydrogen gas in the GED at heating rates (\dot{T}) of 2°C/min, 3°C/min, and 10°C/min. The curves are colored according to the approximate initial gas volume. The average heating rate of the liquid metal and gas for the entirety of each experiment was always within ± 0.4 °C/min of the target heating rate. Similar initial volumes of gas expand in the same manner with increasing temperature, as expected. The effects of different heating rates are difficult to discern from the total expansion measurements. The change in the slope of curves 1 and 2 (hydrogen gas expansion tests) at 560°C supposedly corresponds to the dissolution of hydrogen into the liquid metal, which will be addressed in greater detail later.

As indicated previously, the true gas temperature was assumed to be equivalent to the measured metal temperature. This assumption was valid if the contents of the GED remained reasonably isothermal during heating. The isothermality of the GED's contents was judged according to the difference between the measured glass and metal

temperatures such that

$$\Delta T = T_{glass} - T_m \quad (13)$$

where T_{glass} is the measured exterior glass temperature (at the bottom of the exterior glass thermocouple well). Lower values of ΔT correspond to greater isothermality in the GED, which decreases the error from equating the true gas temperature to the measured metal temperature. In addition, greater isothermality in the GED minimizes the error from assuming that the bonded sand samples and the evolved binder gas are at the same temperature.

Figure 24 shows the measured temperature difference in the GED during the pure gas expansion tests as a function of the measured metal temperature. The curves are colored according to the heating rate. It can be seen that heating the GED at a lower rate decreases the measured GED temperature difference and thereby increases the isothermality of the GED's contents. The isothermality increases with decreasing heating rate because the liquid metal acts as a large thermal mass, and lowering the heating rate reduces the temperature lag of the liquid metal compared to the other contents of the GED. It should be noted that the hydrogen samples heated at a rate of 2°C/min (curves 1 and 2 of Figure 24) are more isothermal than the argon samples heated at the same rate (curves 3-5 of Figure 24). The thermal expansion coefficient of hydrogen is ten times greater than that of argon [37], which causes the hydrogen samples to be more isothermal than the argon samples during heating.

Figure 25 (a-b) illustrates the measured dimensionless molecular weight from select pure argon expansion tests and all hydrogen gas expansion tests plotted as a function of temperature during heating. The dramatic increase in the ratio of measured to known molecular weight for hydrogen above 560°C is presumably due to dissolution of hydrogen into the liquid metal. As previously noted, the gas temperature was assumed to

be equivalent to the measured metal temperature. Figure 25 (a-b) shows that good agreement between the measured and true gas molecular weights is achieved when the gas temperature is approximated as the metal temperature. Additional calculations were performed assuming the gas temperature was equivalent to the measured glass temperature, but the resulting molecular weights were inaccurate. Therefore, equating the gas and metal temperatures was deemed acceptable.

It can be seen in Figure 25 (a-b) that the dimensionless molecular weight measurements draw closer to the ideal value of 1 with increasing temperature (neglecting hydrogen dissolution) and eventually become essentially constant. As the gas volume expands during heating, the sensitivity and accuracy of the molecular weight measurements increase. This is reflected by the differences between the curves in Figure 25 (a). The argon molecular weight curves corresponding to lower initial volumes (curves 1 and 2) experience greater deviation from 1 and are more erratic than the curves corresponding to higher initial volumes (curves 3 and 4) for all temperatures. It is concluded that there is low accuracy in the molecular weight measurements when the change in gas volume is low, and this is especially true at lower temperatures. Therefore, a gas measurement cut-off criterion is imposed. The gas molecular weight measurements are considered reliable when the portion of height change in cylinder 2 from gas expansion Δh_2^g is greater than or equal to 0.8 cm. The gas cut-offs for the pure gas expansion tests are superimposed on the corresponding dimensionless molecular weight curves in Figure 25 (a-b). The molecular weight measurements to the right of the gas cut-off (trusted measurements) for all pure gas expansion tests fall within 5% of the true gas molecular weight. The trusted dimensionless molecular weight measurements also have good repeatability.

Figure 25 (a-b) shows that the greatest deviation of the dimensionless molecular weight from 1 for the argon and hydrogen gases occurs at lower temperatures. This behavior is due to nonisothermality of the GED's contents. The error in the measured

molecular weight is greatest between about 50°C and 150°C, which is the temperature range where the GED experiences the highest amount of nonisothermality as seen in Figure 24. Figure 25 (a) also shows that the error in the molecular weight measurements increases when the heating rate is increased, which is expected because the temperature measurement error in the GED increases with increasing heating rate. It was concluded from these results that the binder gas tests were best performed at a low heating rate of 2°C/min, which would maximize the isothermality of the GED and minimize the error in the molecular weight measurements.

Figure 25 (a-b) indicates that the dimensionless molecular weight for temperatures below 200°C is closer to 1 for the hydrogen tests than for the argon tests. The initial volumes of hydrogen were greater than the initial volumes of argon, which improved the accuracy of the hydrogen molecular weight measurements. As previously stated, the thermal expansion coefficient of hydrogen is ten times greater than that of argon. This caused the hydrogen to be more isothermal than the argon and further improved the accuracy in the hydrogen molecular weight measurements compared to those for argon. These findings further support the decisions to impose a gas measurement cut-off criterion and use a low heating rate of 2°C/min for all binder gas evolution tests.

All measurements of the dimensionless molecular weight from the pure argon gas expansion tests are plotted in Figure 26. The curves are colored according to the heating rate. It can be seen that the error in measuring the molecular weight of small volumes of gas may be as large as 10%. Higher heating rates also tend to decrease the accuracy of the molecular weight measurements. These findings provide additional support for the use of the gas measurement cut-off and a low heating rate of 2°C/min for all binder gas evolution experiments.

4.4 Binder Gas Measurements

The following sub-sections describe the results from the binder gas evolution tests performed using the gas measurement apparatus. The effects of hydrogen dissolution and sand expansion are also addressed. An alternative approach for evaluating the binder gas evolution during heating and cooling is also presented. Finally, the present binder gas molecular weight measurements are compared with the results from previous studies.

4.4.1 Binder Gas Evolution during Heating and Cooling

The measured height change as a function of temperature from all PUNB bonded sand tests performed using the GED are plotted in Figure 27. The heating rate was 2°C/min, and measurements during cooling (dashed lines) are shown when available. The average heating rate of the metal and binder gas for the entirety of each experiment was always within $\pm 0.4^\circ\text{C}/\text{min}$ of the target heating rate. Figure 27 also shows the average metal-only height change for comparison. As expected, decomposition of the PUNB bonded sand generates a significant amount of gas and dramatically increases the measured height change. In general, the height change increases monotonically with temperature. At approximately 585°C, however, the height change rapidly increases and then suddenly decreases with increasing temperature. This substantial peak in the binder gas volume is reproducible and will be addressed in greater detail later in the discussion. After the height change rapidly decreases, it levels out and increases with increasing temperature. The maximum achievable temperature was limited by the maximum allowable height change. The good repeatability in the height change measurements for similar sample masses indicates that the bonded sand samples had homogenous distribution of the binder amongst the particulate matter. It can be seen that the height change during cooling decays linearly for only the 0.637 g and 0.690 g tests. The meaning of this will be addressed later.

The measured binder gas molecular weight curves for all PUNB bonded sand tests

are plotted as a function of temperature in Figure 28. The testing conditions and curve coloring correspond to those of Figure 27, and only gas measurements meeting the gas cut-off criterion ($\Delta h_2^g \geq 0.8$ cm) are plotted. During heating, the binder gas molecular weight rapidly decreases from 375 g/mol at 115°C to 99.8 g/mol at 200°C. The molecular weight is relatively constant until 270°C, after which it decreases at a decreasing rate to 51.6 g/mol at 500°C. After decreasing slightly further above 500°C, the binder gas molecular weight steeply decreases from 47.7 g/mol at 550°C to 30.3 g/mol at 585°C and then steeply increases to 47.2 g/mol at 630°C. This steep decrease and increase in the binder gas molecular weight measurements corresponds to the peak in the height change measurements. The molecular weight remains essentially constant from 630°C to 750°C. No additional binder gas mass is generated at temperatures greater than 710°C. Above 750°C, the binder gas molecular weight gradually decreases to 33.3 g/mol at 898°C, indicating that the binder gas components continue to react with each other after the solid binder decomposition is complete.

It can be seen from Figure 28 that the molecular weight measurements have excellent repeatability across the entire temperature range. It is also important to note how the molecular weight curves from different experiments agree at 300°C. The volume of gas evolved from the larger masses of bonded sand is significant by 300°C, which ensures that the corresponding molecular weight measurements at this temperature are accurate. Figure 28 shows that the gas measurement cut-off (i.e., the point where the molecular weight measurements become reliable) when smaller amounts of bonded sand are employed corresponds to temperatures near 300°C. The good agreement between the binder gas molecular weight measurements at 300°C for different amounts of bonded sand proves that the imposed gas measurement cut-off provides an effective means to differentiate between reliable and unreliable binder gas molecular weight measurements.

TGA of PUNB bonded sand during cooling was not performed. When cooling measurements were recorded during the gas measurement tests, the binder gas mass at the

test's maximum temperature was assumed to be constant throughout the cooling portion of the test. This assumption is valid only if the binder gas does not condense during cooling. Data are not available to accurately calculate the binder gas molecular weight if condensation occurs. Figure 28 shows binder gas molecular weight measurements during cooling for tests that clearly exhibited no binder gas condensation (dashed lines). It can be seen that the binder gas does not condense during cooling when the bonded sand is previously heated above 709°C.

The estimated error in the measurement of the binder gas molecular weight during heating was determined through a detailed root-sum-squares error analysis. The primary sources of error in the binder gas molecular weight measurements are shown in Table 5, with average values reported for parameters that are temperature-dependent (f and β_m^{eff}). The significance of each primary error source on the molecular weight measurements is related to the total initial PUNB bonded sand sample mass and the measurement temperature. For example, when the bonded sand sample mass is large, more binder gas mass is generated and the error in the fraction of original binder mass remaining has a greater impact on the molecular weight measurements. More binder gas generation also results in larger volumes of binder gas, which influences the accuracy of the molecular weight measurements as previously discussed. Also, the volume of gas generated when a given temperature is reached depends on the sample size. The average error in the present binder gas molecular weight measurements between 115°C and 898°C is estimated to be 6%.

As previously indicated, the measured gas mass evolution from PUNB bonded sand is relatively the same for heating rates of 2°C/min, 10°C/min, and 100°C/min. Therefore, it is speculated that the binder gas molecular weight measured during heating of PUNB bonded sand at a rate of 2°C/min should roughly correspond to the molecular weight of gas evolved from PUNB bonded sand during heating at rates between 2°C/min and 100°C/min. Due to the similarities in the bonding chemistry between PUCB and

PUNB binder systems, it is speculated that the measured molecular weight of gas evolved from PUNB bonded sand should also roughly correspond to the molecular weight of gas evolved from PUCB bonded sand.

4.4.2 Effects of Hydrogen Dissolution on the Binder Gas

Molecular Weight Measurements

It was hypothesized that the dramatic peak in the molecular weight measurements at about 585°C was due to the effects of hydrogen dissolution into the liquid metal. Figure 25 (b) clearly shows that hydrogen dissolution does not cause any peak in the measured molecular weight of pure hydrogen gas. In addition, the binder gas composition data shown in Table 1 indicate that hydrogen evolution is insignificant at temperatures near 750°C. This further supports the conclusion that the peak in the measured molecular weight is not due to hydrogen dissolution. Regardless of these facts, the possible issue of hydrogen dissolution during heating and its potential effects on the measured binder gas molecular weight were investigated further.

Equations 9 and 10 for pure hydrogen gas were modified and combined such that the ratio of measured to known molecular weight can be written as

$$\phi = \frac{(m_g + m_g^d)}{M_{H_2}} \left(\frac{\bar{R}T}{P_g V_g} \right) \quad (14)$$

where the initial mass of gas was found using Equation 9 combined with the initial measurements of the hydrogen gas, and m_g^d is the dissolved gas mass. The dissolved gas mass as a function of temperature was found by solving Equation 14 with $\phi = 1$. Analysis of Figure 25 (b) reveals that the slope changes of the hydrogen ϕ curves are essentially the same above 560°C. This implies that the temperature-rates of pure hydrogen mass loss from dissolution into the liquid metal during heating above 560°C are approximately the same. As a worst-case estimation, it was assumed that binder gas

hydrogen dissolves into the liquid metal at the average rate determined from the pure hydrogen expansion tests, regardless of the actual volume of binder gas hydrogen. The temperature-rate of hydrogen mass loss averaged from the pure hydrogen tests was applied to a discretized Taylor series. This allowed the mass of hydrogen gas dissolved into the liquid metal to be approximated at a given temperature point i during heating of any volume of hydrogen above 560°C. The approximated mass of dissolved hydrogen gas was derived as

$$m_g^{d*} = \begin{cases} 0 & T^i < 560^\circ\text{C} \\ m_g^{d*}(T^{i-1}) + \frac{dm_g^d}{dT}(T^i) \cdot [T^i - T^{i-1}] & T^i \geq 560^\circ\text{C} \end{cases} \quad (15)$$

where m_g^{d*} is evaluated at the temperature point T^{i-1} and dm_g^d/dT is evaluated at the temperature point T^i . The volume of gas corresponding to the mass of binder gas hydrogen that “hypothetically” dissolved during heating was added back into the system. This was done by modifying the measured height change in cylinder 2 to account for the additional gas volume change from the hydrogen correction. The resulting corrected total height change in cylinder 2 of the GED was found as

$$\Delta h_2^c = \Delta h_2 + \frac{4}{\pi D_2^2} \left(\frac{m_g^{d*} \bar{R} T}{M_{\text{H}_2}^0 P_g} \right) \quad (16)$$

The total height change with the hydrogen dissolution correction was then used to calculate corrected values for the gas volume, pressure, and binder gas molecular weight as a function of temperature during heating. The corrected and uncorrected binder gas molecular weight measurements during heating of a 0.637 g PUNB bonded sand sample at a rate of 2°C/min are compared in Figure 29, and only gas measurements meeting the gas cut-off criterion ($\Delta h_2^g \geq 0.8$ cm) are plotted. On a worst-case basis, hydrogen dissolution during heating changes the molecular weight readings above 560°C by a maximum of about 4 g/mol. Since hydrogen is not expected to significantly evolve within

the temperature range of the present measurements (see Table 1) and hydrogen dissolution does not dramatically affect the molecular weight measurements, the above described hydrogen dissolution correction of the measured binder gas molecular weight was discarded.

4.4.3 Effects of Sand Expansion on the Binder Gas

Molecular Weight Measurements

It was also hypothesized that the dramatic peak in the binder gas molecular weight measurements at 585°C was related to the volume change in the silica sand, caused by the increase in thermal expansion accompanying the sand's α - β phase transformation at 573°C [38]. An additional experiment was performed to evaluate this hypothesis. The expansion of 1.018 g of pure IC55 silica sand, 3.8 cm³ of argon, and the liquid metal in the GED was measured during heating at a rate of 2°C/min. The dimensionless molecular weight measurements of the argon and sand mixture along with other corresponding measurements for pure argon are illustrated in Figure 30, and only gas measurements meeting the gas cut-off criterion ($\Delta h_2^g \geq 0.8$ cm) are plotted. The argon and sand molecular weight measurements are within 5% of those for pure argon until about 400°C. The decrease in the argon and sand molecular weight between 400°C and 600°C indicates that a small amount of gas is generated from decomposition of the pure sand. Again, this gas generation is minor compared to the amount of gas evolved from binder decomposition. No additional gas is evolved from the pure sand above 600°C. It is quite clear from Figure 30 that no peak in the molecular weight measurements occurs when argon and sand are heated in the GED.

4.4.4 Additional Analysis of the Measured Peak in the

Binder Gas Molecular Weight during Heating

It is possible that the peak in the measured binder gas molecular weight is caused by a reaction between the binder gas and the sand. However, it is more likely that the

peak simply reflects the actual binder gas evolution behavior. It can be seen from Figure 15 (b) that the bonded sand fraction of original binder mass does not experience any unusual behavior at 585°C. This implies that the peak in the measured binder gas molecular weight may correspond to the rapid release of low molecular weight compounds followed by the release of high molecular weight compounds during heating at temperatures near 585°C. Recall, however, that the binder gas evolved during TGA of bonded sand was removed from the sample area, while the bonded sand samples in the GED were immersed in the evolved binder gas. Therefore, it is also possible that the presence of both the evolved binder gas and the bonded sand influences the manner in which additional gas is evolved from the bonded sand or the manner in which the previously evolved binder gas components react with one another during heating at temperatures near 585°C.

4.4.5 Molar Evolution of the Binder Gas during Heating and Cooling

Binder gas condensation prevented most of the binder gas molecular weight measurements during cooling from being properly analyzed. It was desirable to determine a method for directly comparing the measured binder gas evolution during heating and cooling. The moles of evolved binder gas per original binder mass were calculated by

$$n_b = \frac{m_b/M_b}{m_s^0 \chi/100} \quad (17)$$

The moles of evolved binder gas per original binder mass describes the gas evolution behavior regardless of the actual binder gas mass, thereby allowing for direct comparison of the gas evolution during heating and cooling. The moles of binder gas evolved per original binder mass for all binder gas evolution tests are plotted as a function of temperature in Figure 31. Again, the testing conditions and curve coloring correspond to

those of Figure 27, and only data meeting the gas cut-off criterion ($\Delta h_2^g \geq 0.8$ cm) are plotted. A significant decrease in the evolved binder gas moles per original binder mass during cooling indicates condensation of the binder gas. As shown in Figure 31, the binder gas does not condense during cooling when the bonded sand is previously heated to temperatures above 709°C. However, heating the PUNB bonded sand samples to temperatures lower than about 507°C results in partial condensation of the binder gas during cooling at approximately 165°C.

4.4.6 Comparison of the Present Molecular Weight

Measurements with the Results from Previous Studies

The present binder gas molecular weight measurements were fit to a set of piecewise polynomials. The present molecular weight measurements were also extrapolated to higher temperatures based on the average molecular weights calculated using the binder gas composition data from References [17-20], and a final polynomial was fit to this extrapolation. The molecular weight polynomial curves and the binder gas molecular weights calculated from the data of References [17-23] are plotted as a function of temperature in Figure 32. The equations for the binder gas molecular weight polynomials are listed in Table 6. Figure 32 shows that the decreasing behavior of the present molecular weight measurements near 898°C is consistent with the high temperature molecular weight data calculated from References [17-20]. Following the extrapolated curve, it is expected that the binder gas molecular weight continues to decrease with increasing temperature from 898°C to 1350°C, after which the molecular weight is approximately constant at about 17.4 g/mol. In general, the present binder gas molecular weight measurements are consistent with molecular weights calculated from the composition data from References [22] and [23], aside from the high molecular weight of 137 g/mol at 500°C (932°F) that appears to be an outlier.

The measured variation in the binder gas molecular weight with temperature also

reflects portions of the binder's thermal degradation mechanism during heating. Giese *et al.* [39] used differential scanning calorimetry (DSC) to measure the energy released from pure PUNB binder samples (60:40 ratio of Part 1 to Part 2) during heating at a rate of 10°C/min. The various peaks in the DSC curve were associated with specific physical or chemical changes in the binder. Figure 32 shows a portion of the solid binder's thermal degradation mechanism superimposed on the fit of the present binder gas molecular weight measurements. The breaking of the binder's urethane bonds corresponds with the plateau in the molecular weight between 200°C and 280°C. The breakdown of the binder to polymer aromatics coincides with the decrease in the binder gas molecular weight between 280°C and 400°C. The binder's thermal degradation mechanism above 400°C is undetermined.

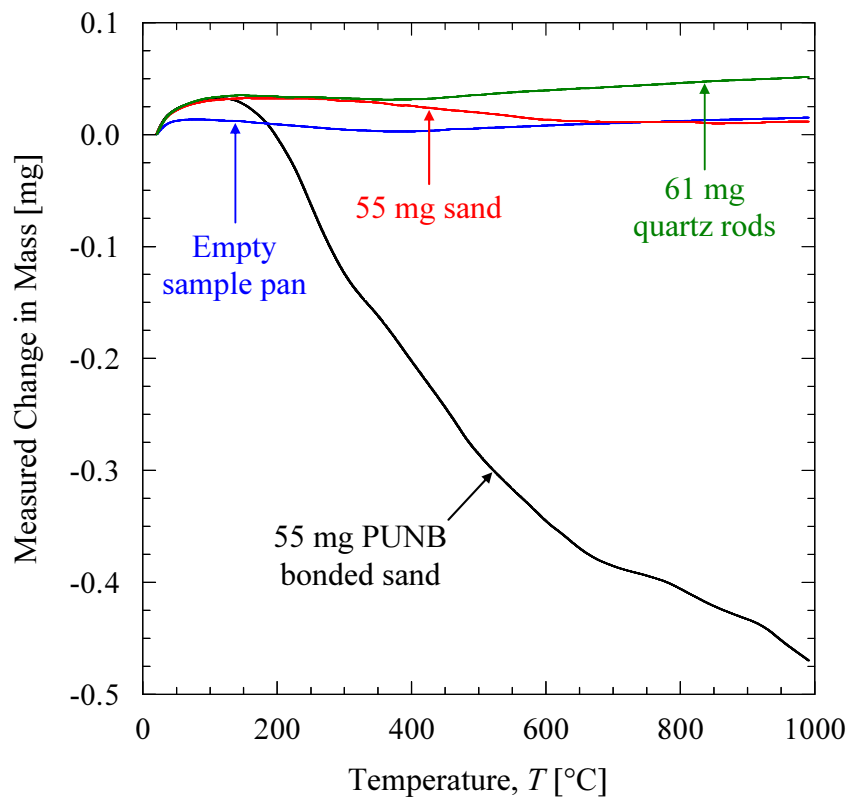


Figure 10: Measured change in mass as a function of temperature typical of PUNB bonded sand samples, pure IC55 silica sand samples, the empty sample pan, and quartz rods during heating at a rate of $100^{\circ}\text{C}/\text{min}$ with a total argon gas flow of $80\text{ cm}^3/\text{min}$.

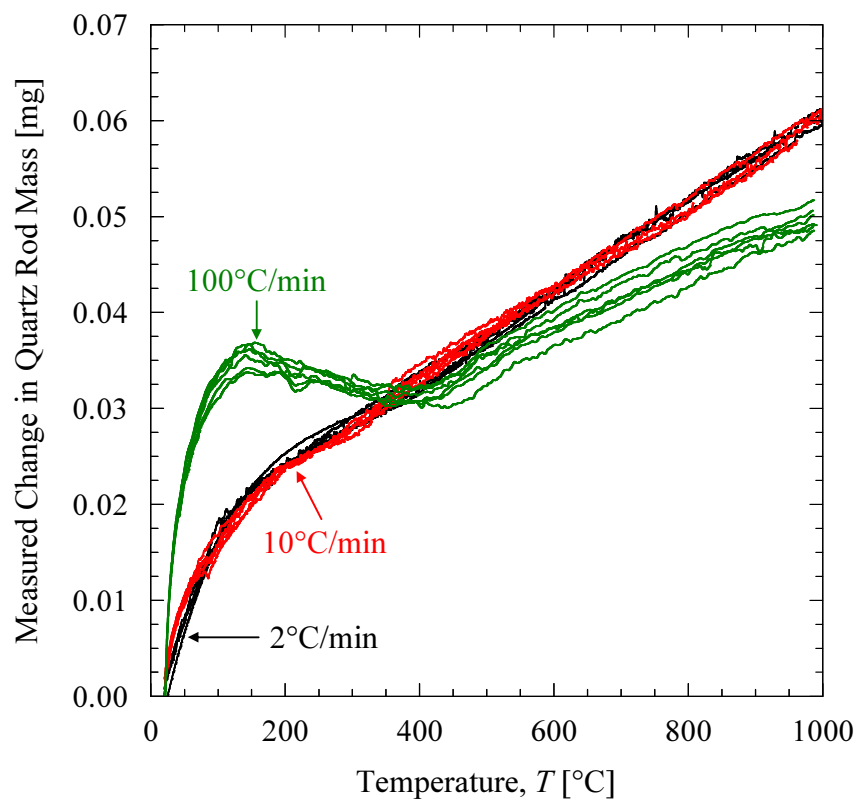


Figure 11: Measured change in the mass of quartz rods as a function of temperature during heating at rates of $2^{\circ}\text{C}/\text{min}$, $10^{\circ}\text{C}/\text{min}$, and $100^{\circ}\text{C}/\text{min}$. The quartz rods had a total mass of 61 mg, and the measurements were unaffected by argon flow rate.

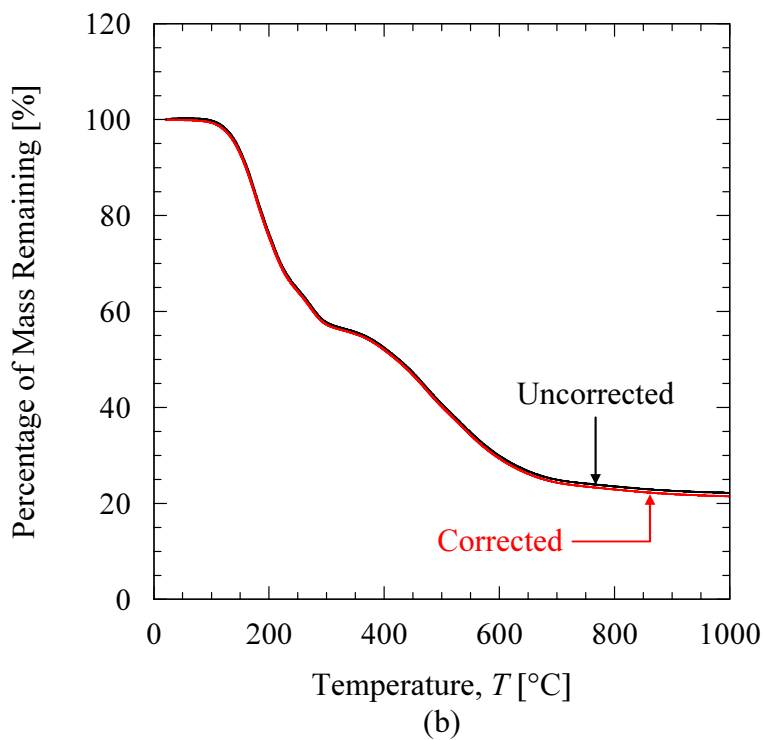
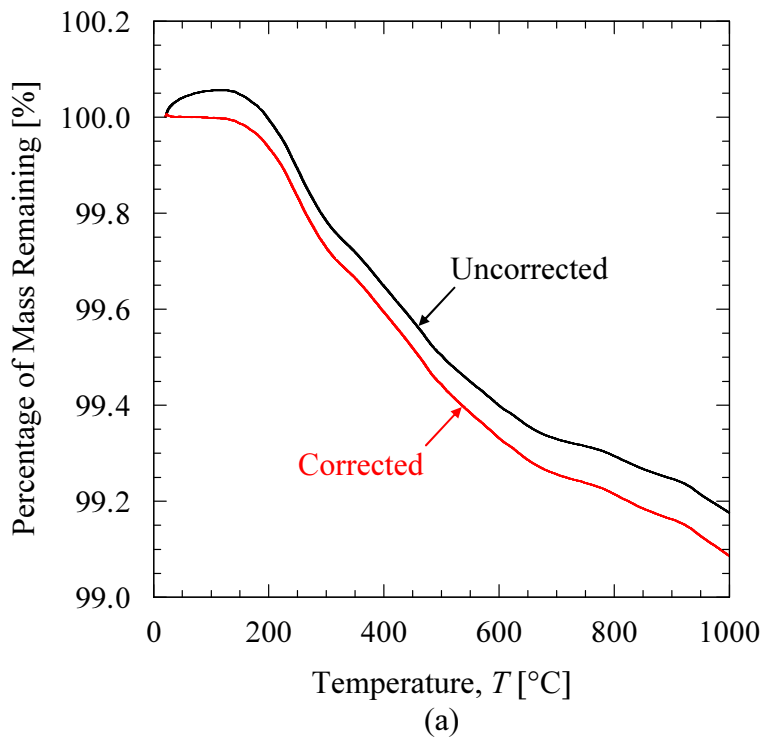


Figure 12: Comparison of the uncorrected and corrected percentage of mass remaining as a function of temperature in (a) 55 mg PUNB bonded sand samples and (b) 7.5 mg pure PUNB binder samples during heating at a rate of $100^{\circ}\text{C}/\text{min}$ with a total argon gas flow of $80\text{ cm}^3/\text{min}$.

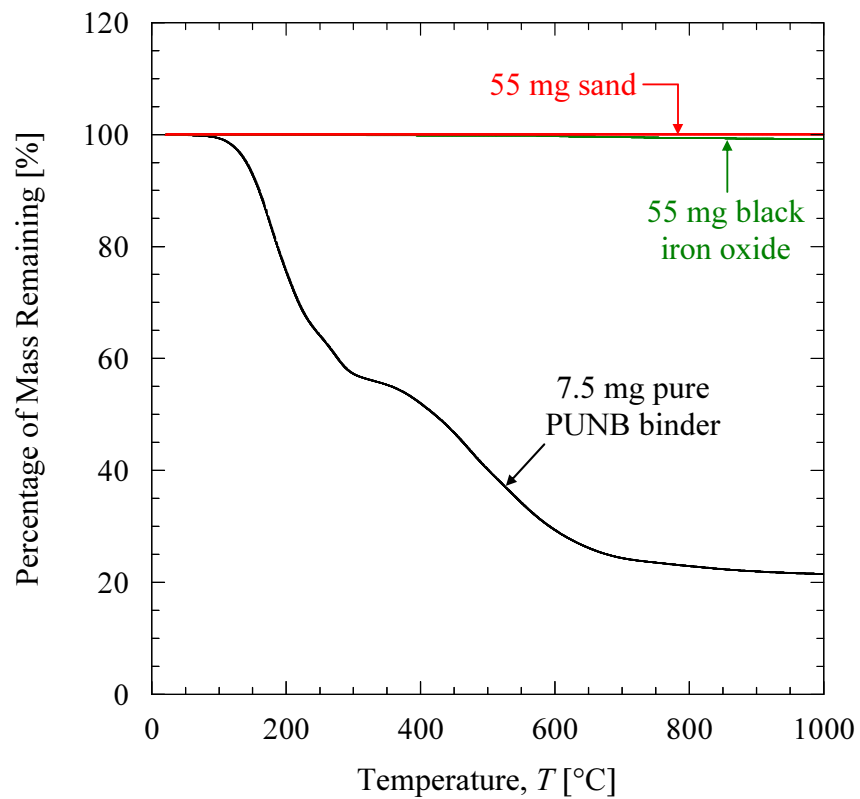


Figure 13: Measured percentage of mass remaining in the individual components of PUNB bonded sand as a function of temperature during heating at a rate of $100^{\circ}\text{C}/\text{min}$ with a total argon gas flow of $80\text{ cm}^3/\text{min}$. More than 91% of the mass loss in PUNB bonded sand during heating is due to binder decomposition.

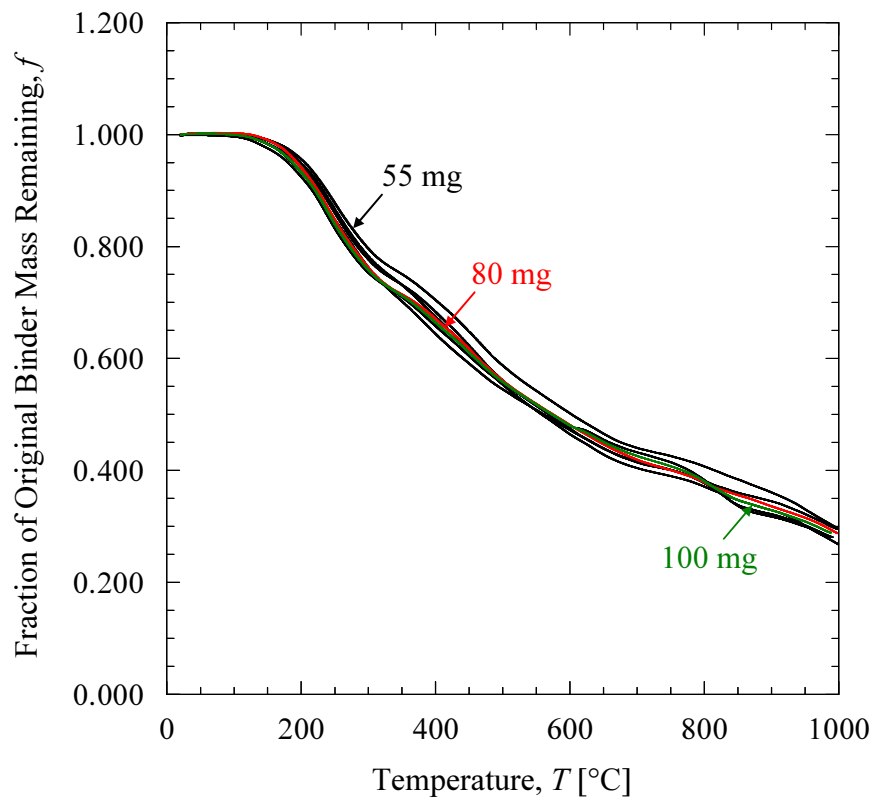


Figure 14: Measured fraction of original binder mass remaining in various masses of PUNB bonded sand as a function of temperature during heating at a rate of 100°C/min with a total argon gas flow of 80 cm³/min. Increasing the bonded sand sample mass from 55 mg to 80 mg or 100 mg does not affect the results.

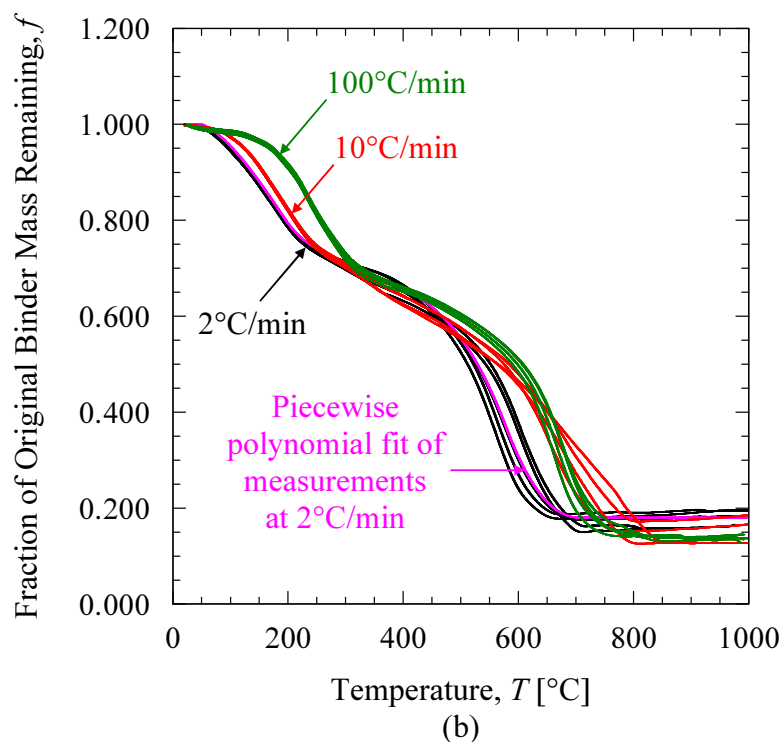
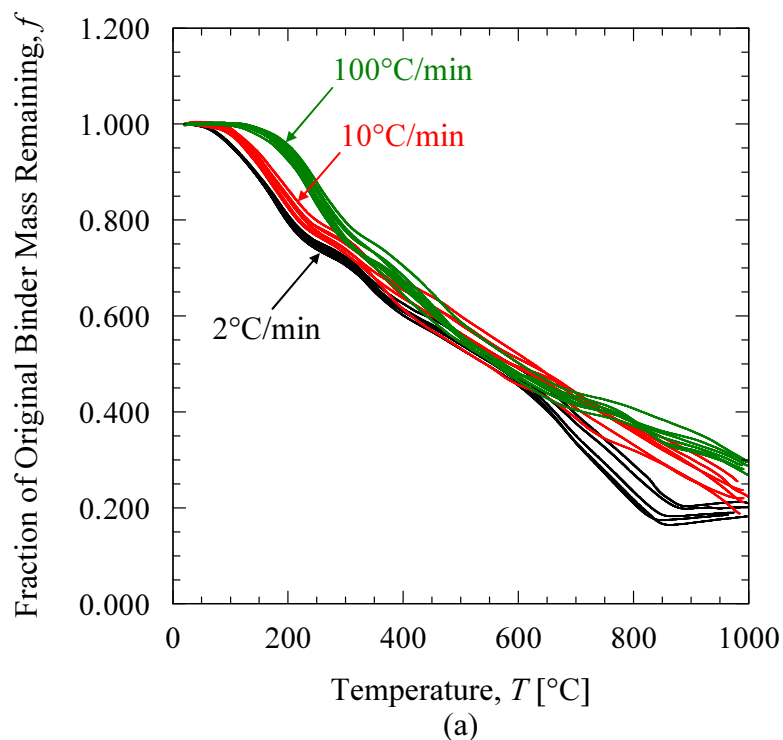


Figure 15: Measured fraction of original binder mass remaining in 55 mg PUNB bonded sand samples as a function of temperature during heating at rates of 2°C/min, 10°C/min, and 100°C/min with total argon gas flow rates of (a) 80 cm³/min and (b) 25 cm³/min. The piecewise polynomial fitted to the measurements for 2°C/min with 25 cm³/min of gas flow is also illustrated.

Table 4: Piecewise polynomial fitted to the measurements of the fraction of original binder mass remaining in bonded sand samples during TGA pyrolysis at a heating rate of 2°C/min with a total argon flow rate of 25 cm³/min.

Fraction of Original Binder Mass Remaining, f	Temperature, T [°C]
1.000	$T \leq 50$
$2.067 \times 10^{-8} T^3 - 1.189 \times 10^{-5} T^2 + 5.036 \times 10^{-4} T + 1.002$	$50 < T \leq 200$
$-6.269 \times 10^{-8} T^3 + 5.148 \times 10^{-5} T^2 - 1.465 \times 10^{-2} T + 2.165$	$200 < T \leq 300$
$-1.711 \times 10^{-8} T^3 + 1.793 \times 10^{-5} T^2 - 6.747 \times 10^{-3} T + 1.583$	$300 < T \leq 580$
$-1.353 \times 10^{-8} T^3 + 3.876 \times 10^{-5} T^2 - 3.446 \times 10^{-2} T + 9.951$	$580 < T \leq 710$
0.1807	$T > 710$

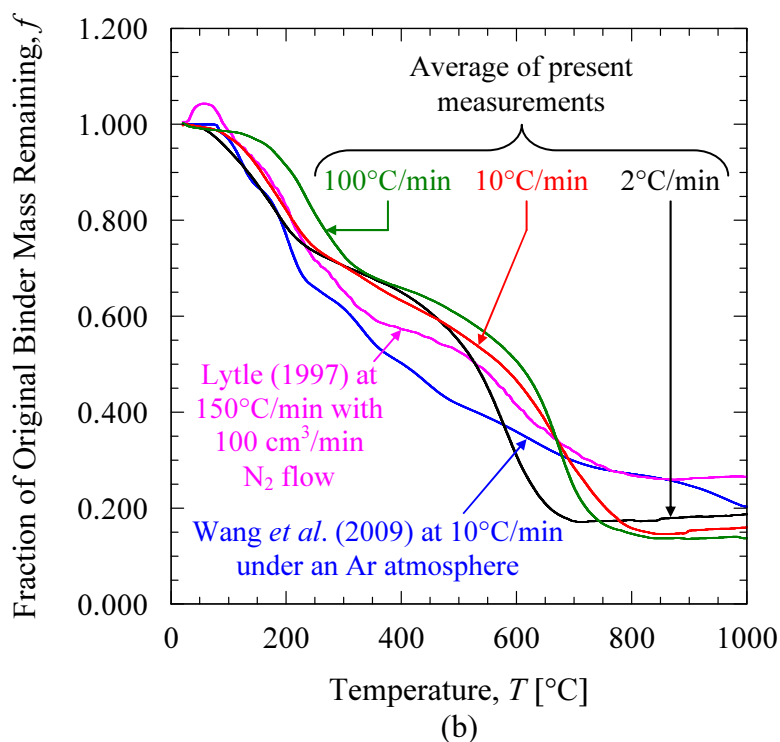
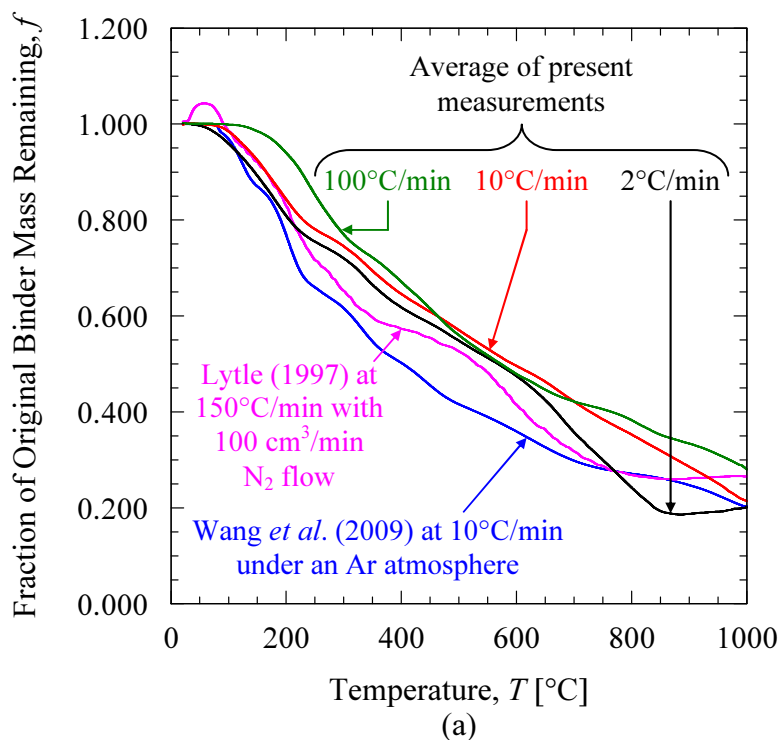


Figure 16: Comparison of the fraction of original binder mass remaining in bonded sand samples as a function of temperature during heating from the present PUNB measurements (averaged) using total argon flow rates of (a) 80 cm³/min and (b) 25 cm³/min with the fractions calculated from TGA data of previous studies. Lytle [23] and Wang *et al.* [24] both tested 1.5% PUCB bonded sand.

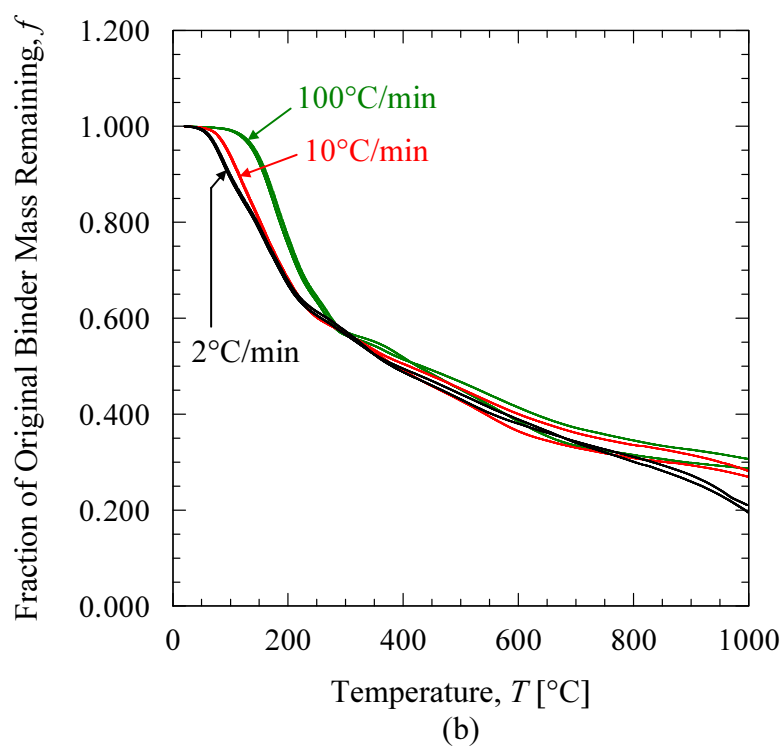
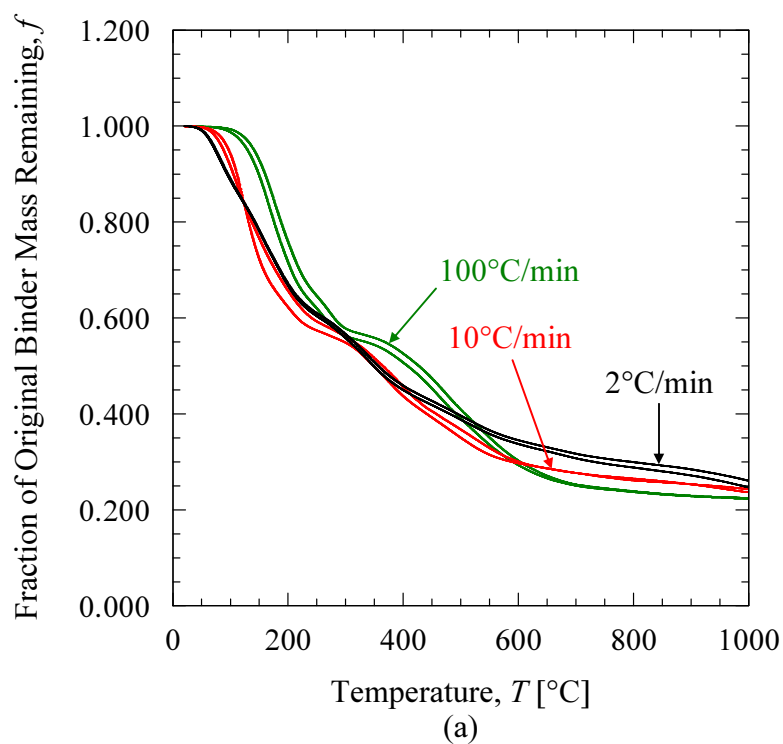


Figure 17: Measured fraction of original binder mass remaining in 7.5 mg pure PUNB binder samples as a function of temperature during heating at rates of $2^{\circ}\text{C}/\text{min}$, $10^{\circ}\text{C}/\text{min}$, and $100^{\circ}\text{C}/\text{min}$ with total argon gas flow rates of (a) $80\text{ cm}^3/\text{min}$ and (b) $25\text{ cm}^3/\text{min}$.

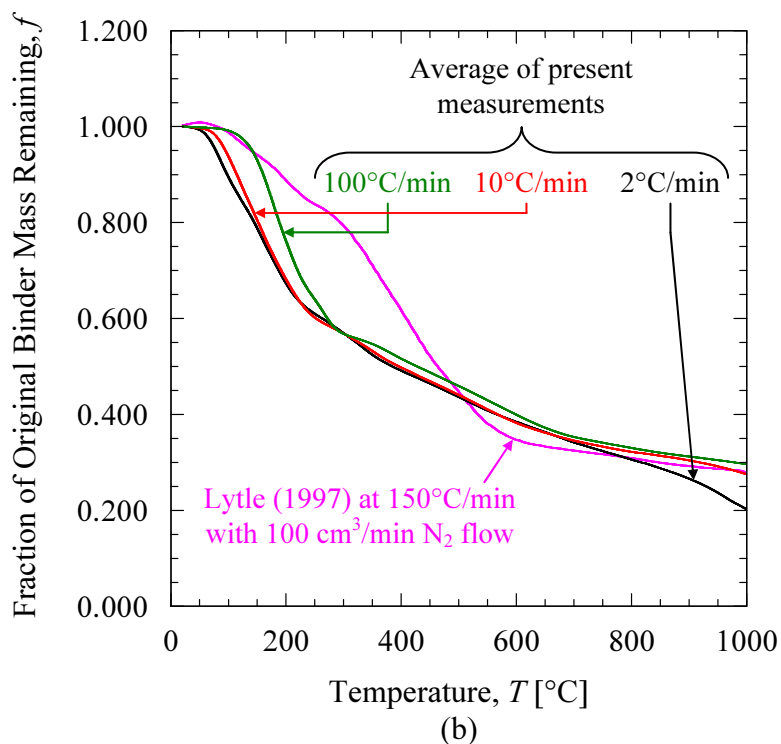
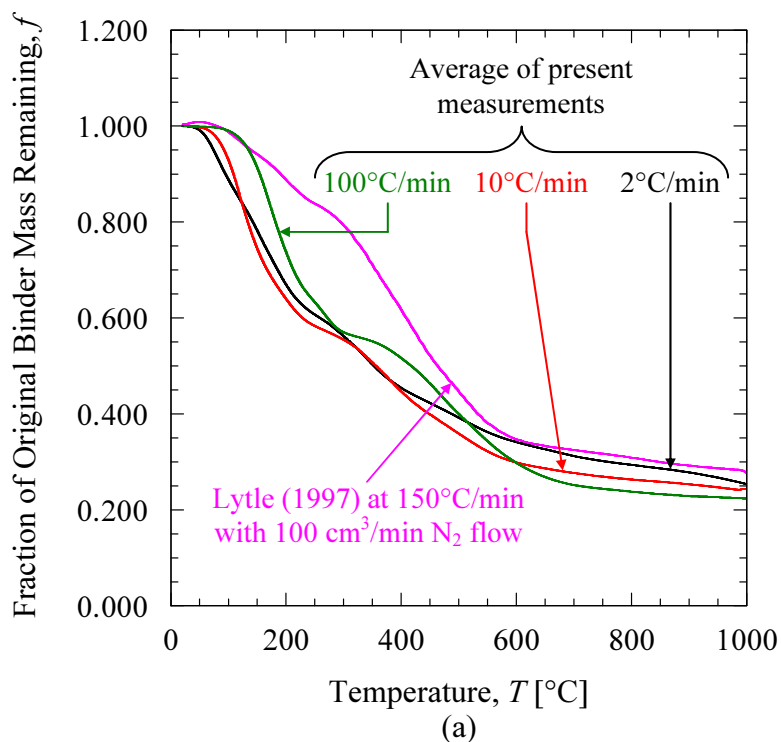


Figure 18: Comparison of the fraction of original binder mass remaining in pure binder samples as a function of temperature during heating from the present PUNB measurements (averaged) using total argon gas flow rates of (a) 80 cm³/min and (b) 25 cm³/min with the fraction calculated from TGA data of Lytle [23] for pure PUCB binder with a 55:45 ratio of Part 1 to Part 2.

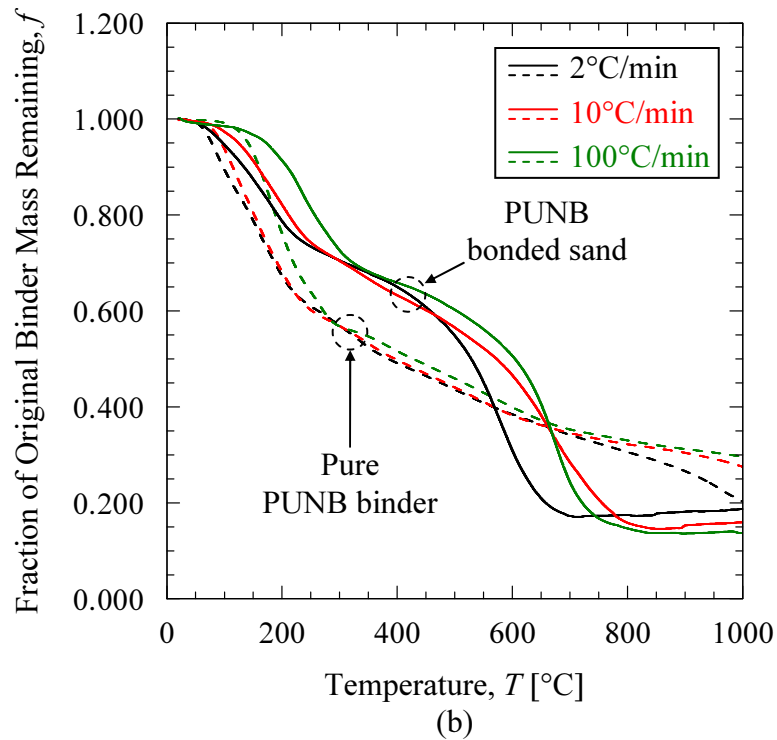
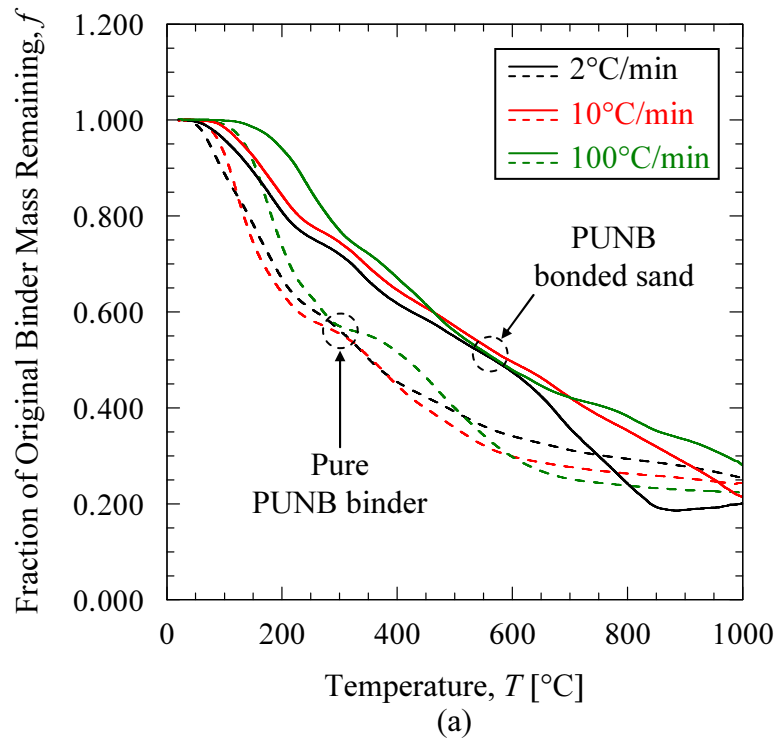


Figure 19: Comparison of the average fraction of original binder mass remaining in 55 mg PUNB bonded sand and 7.5 mg pure PUNB binder samples as a function of temperature during heating at rates of 2°C/min, 10°C/min, and 100°C/min with total argon gas flow rates of (a) 80 cm³/min and (b) 25 cm³/min.

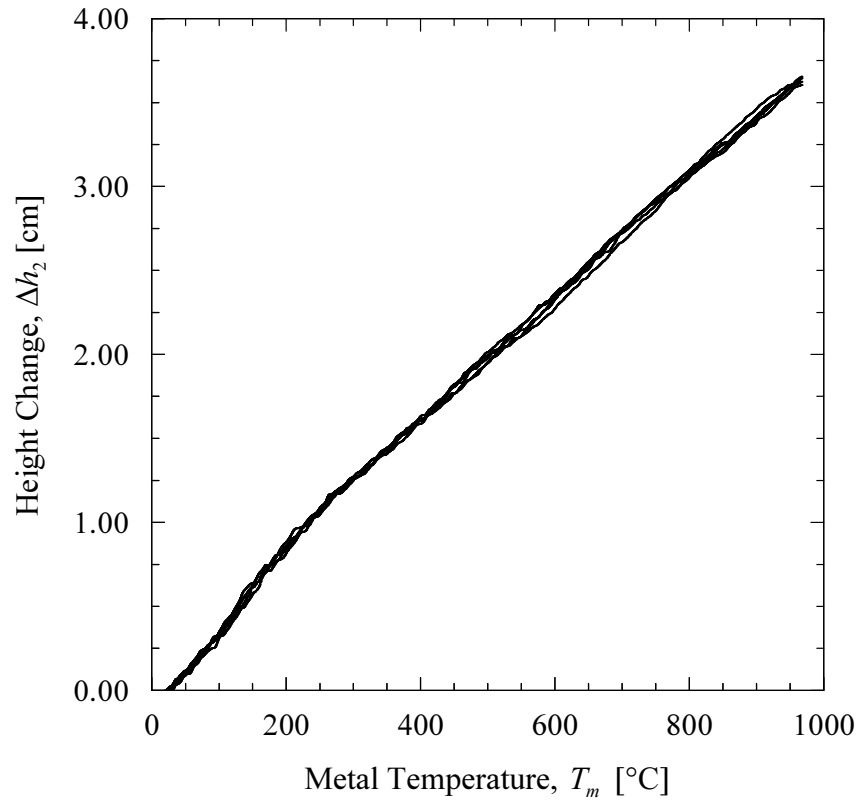


Figure 20: Measured metal-only height change in the GED as a function of temperature during heating at constant rates ranging from 2°C/min to 15°C/min.

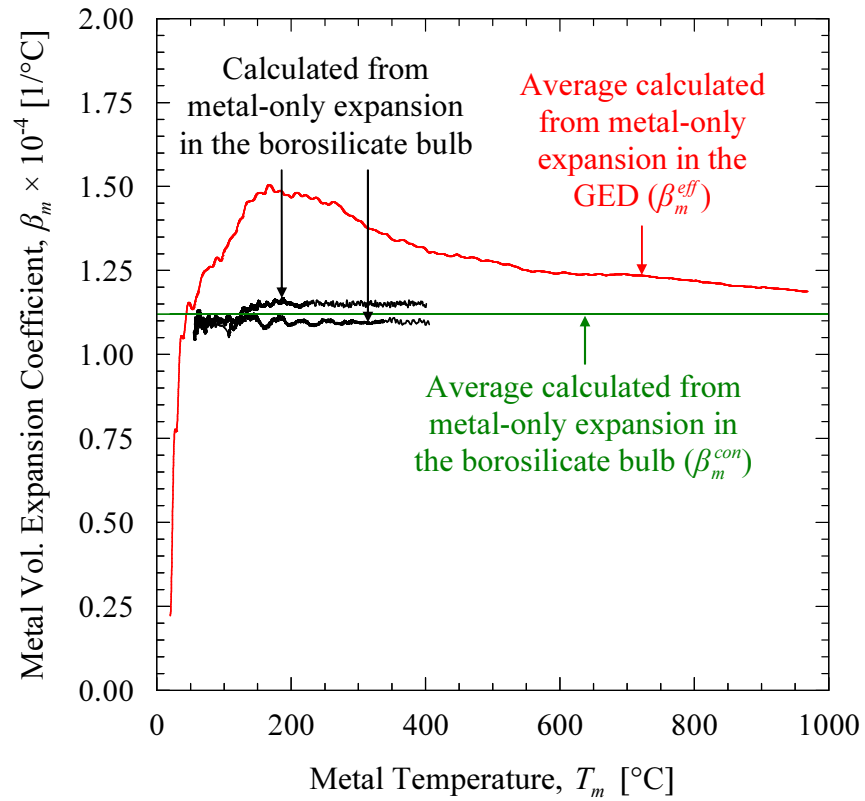


Figure 21: Liquid metal volumetric expansion coefficients calculated from metal-only expansion in the GED and the borosilicate bulb as a function of temperature during heating.

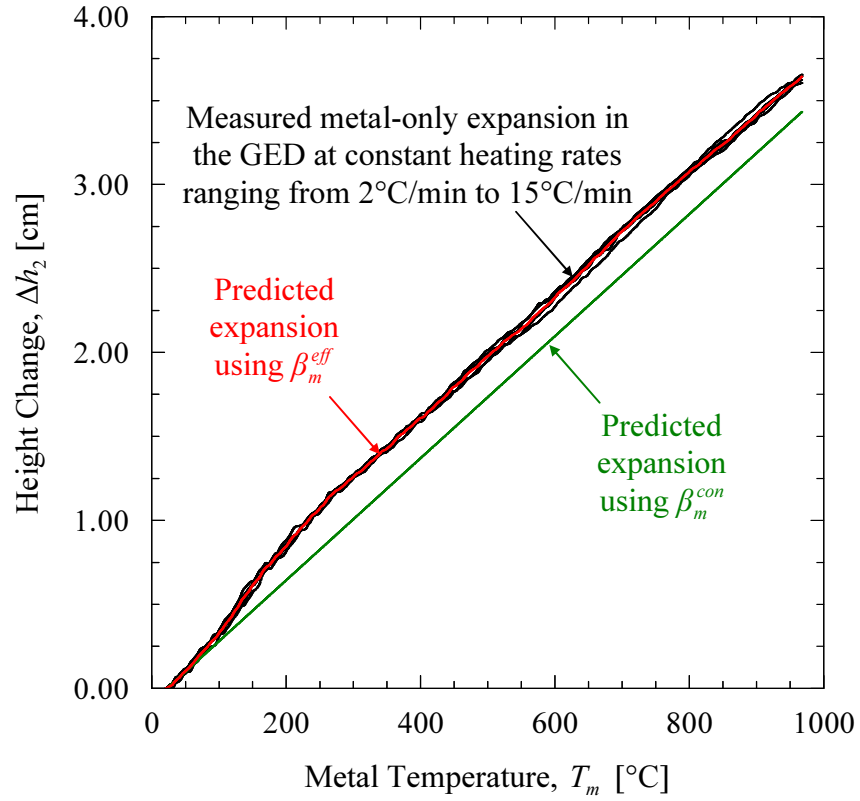


Figure 22: Comparison of measured and predicted metal-only height change in the GED as a function of temperature during heating.

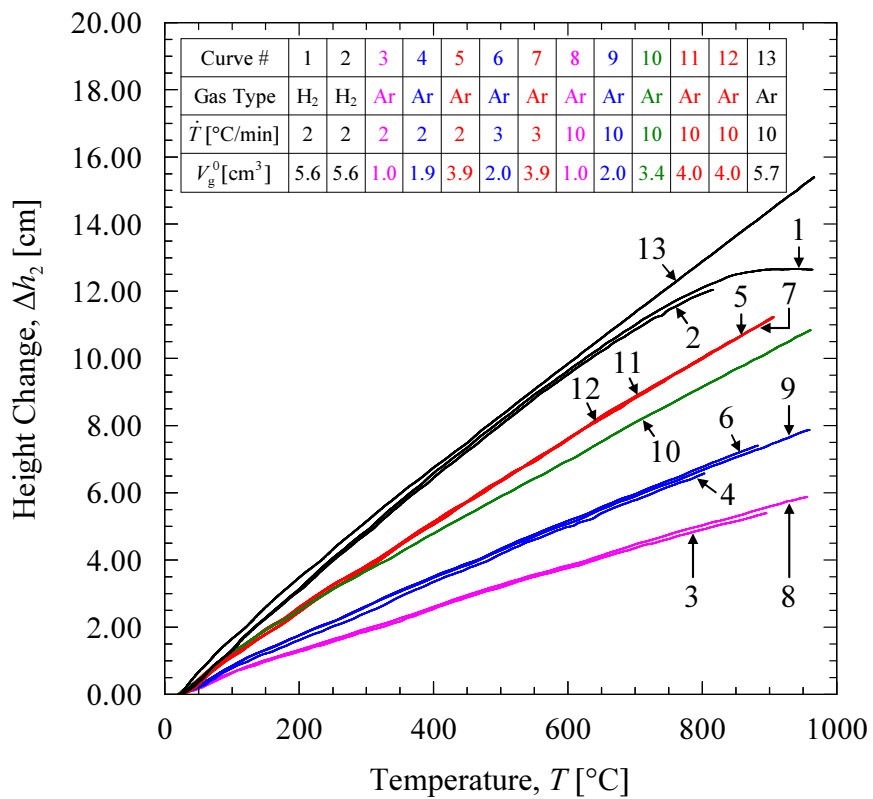


Figure 23: Measured height change as a function of temperature for all pure gas expansion tests in the GED. The curves are colored according to the approximate initial gas volume.

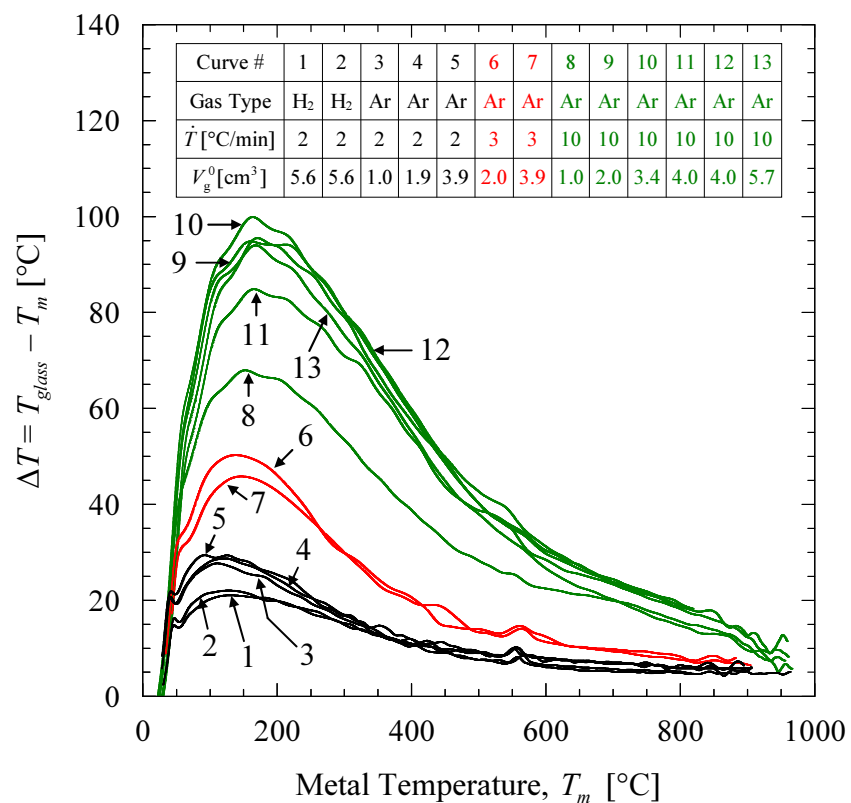


Figure 24: Measured temperature difference in the GED's thermocouple wells as a function of metal temperature for all pure gas expansion tests during heating. The curves are colored according to the heating rate. Smaller values of ΔT imply greater isothermality in the GED's contents, resulting in more accurate measurements of the sample gas's molecular weight.

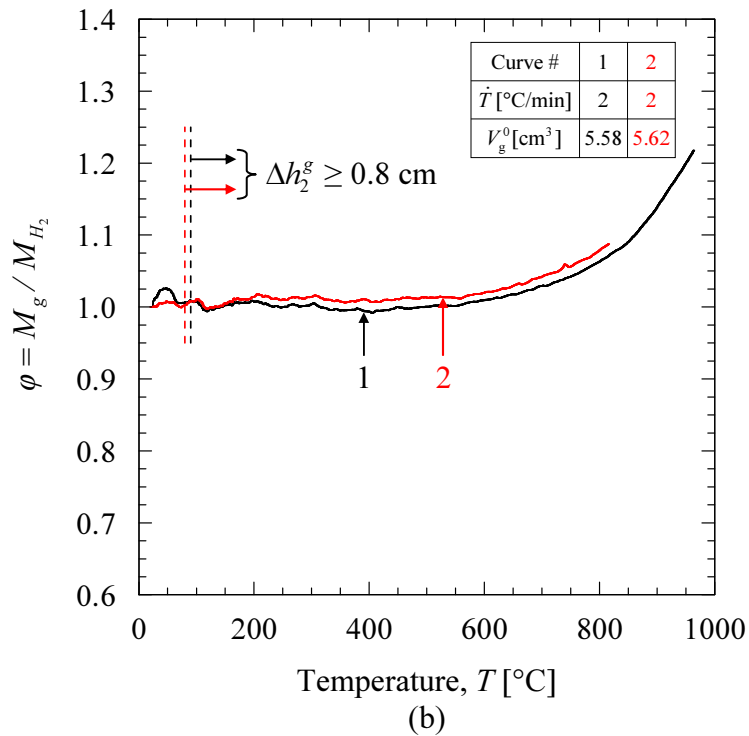
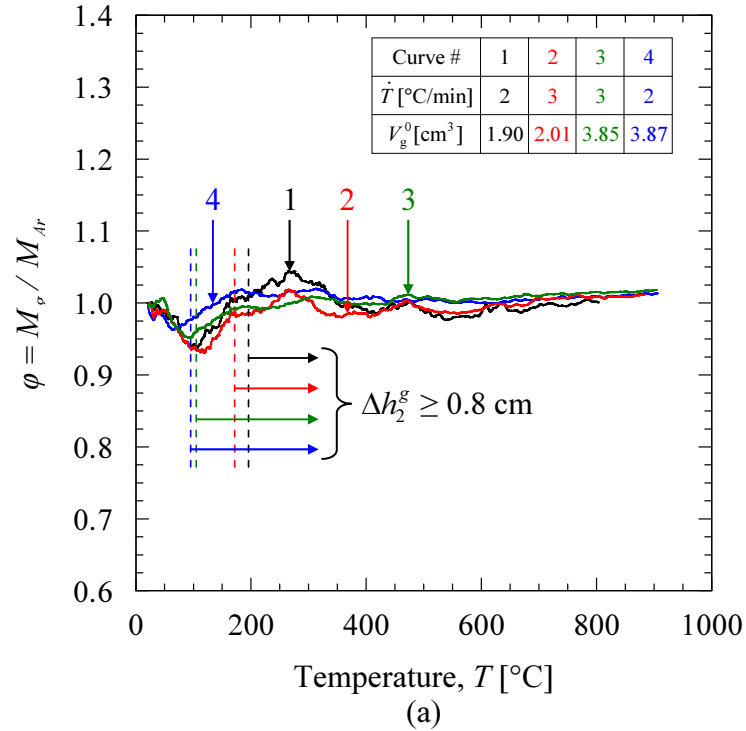


Figure 25: Ratio of measured to known molecular weight of (a) argon gas and (b) hydrogen gas as a function of temperature during heating. The illustrated argon results were selected from many argon expansion tests to provide a clear comparison. The increase in ϕ above 560°C for the pure hydrogen tests is presumably due to dissolution of the hydrogen gas into the liquid metal.

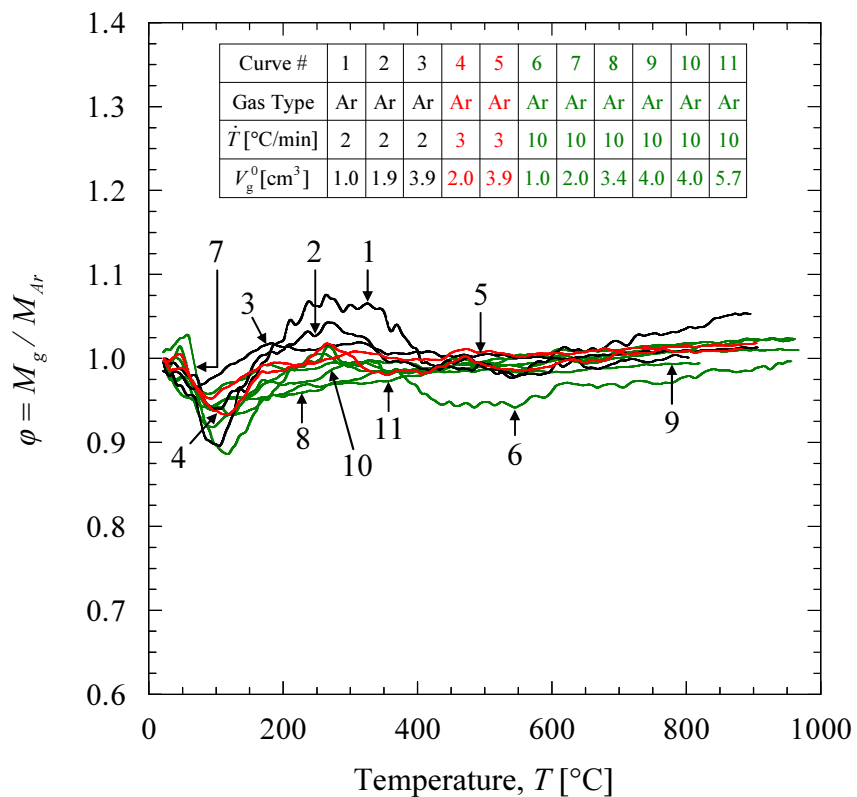


Figure 26: Ratio of measured to known molecular weight of argon gas from all pure argon gas expansion tests as a function of temperature during heating. The curves are colored according to the heating rate.

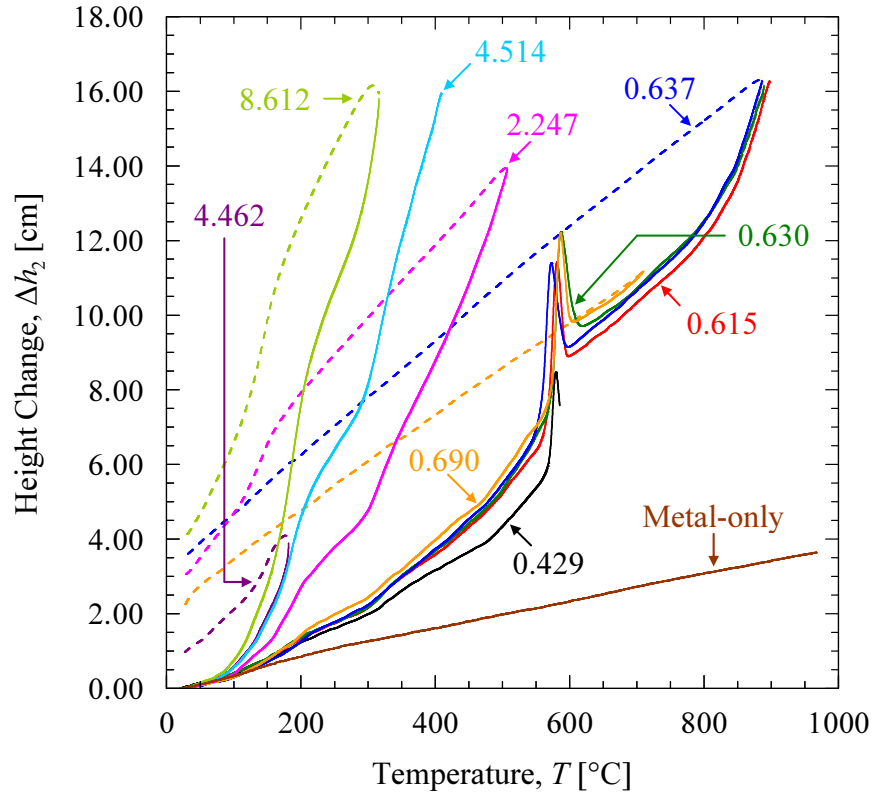


Figure 27: Measured height change as a function of temperature during heating and cooling of different PUNB bonded sand sample masses. Solid lines indicate heating at a rate of 2°C/min, and dashed lines indicate cooling after the furnace was turned off. The average metal-only expansion results are shown for comparison.

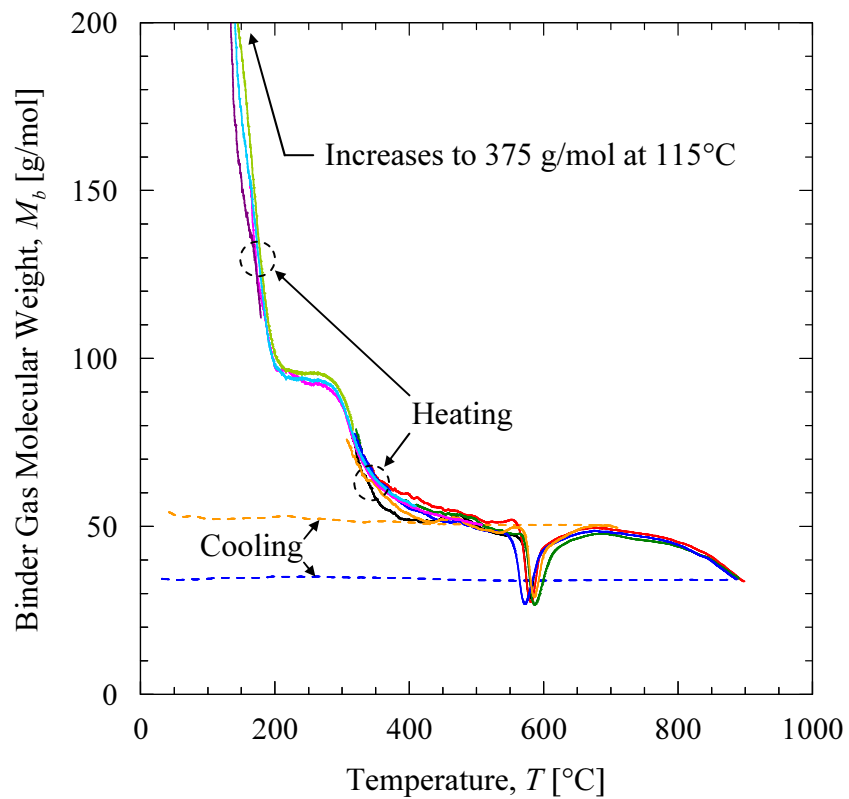


Figure 28: Binder gas molecular weight measurements as a function of temperature during heating and cooling of different PUNB bonded sand sample masses. The color scheme of the curves follows that of Figure 27. The heating rate is 2°C/min, and measurements during cooling are shown for tests that clearly exhibited no binder gas condensation.

Table 5: Primary sources of error in the binder gas molecular weight measurements.

Source of Error	\pm Error
Fraction of Original Binder Mass Remaining, f	0.012
Measured Metal Height Change in Cylinder 2, Δh_2 [cm]	0.05
Liquid Metal Density at Room Temperature, ρ_m^0 [g/cm ³]	0.018
Effective Volumetric Expansion Coefficient of Liquid Metal, β_m^{eff} [1/°C]	0.00001
Volume Contained by the Filled GED at the Initial Temperature, V_{fill}^0 [cm ³]	0.05

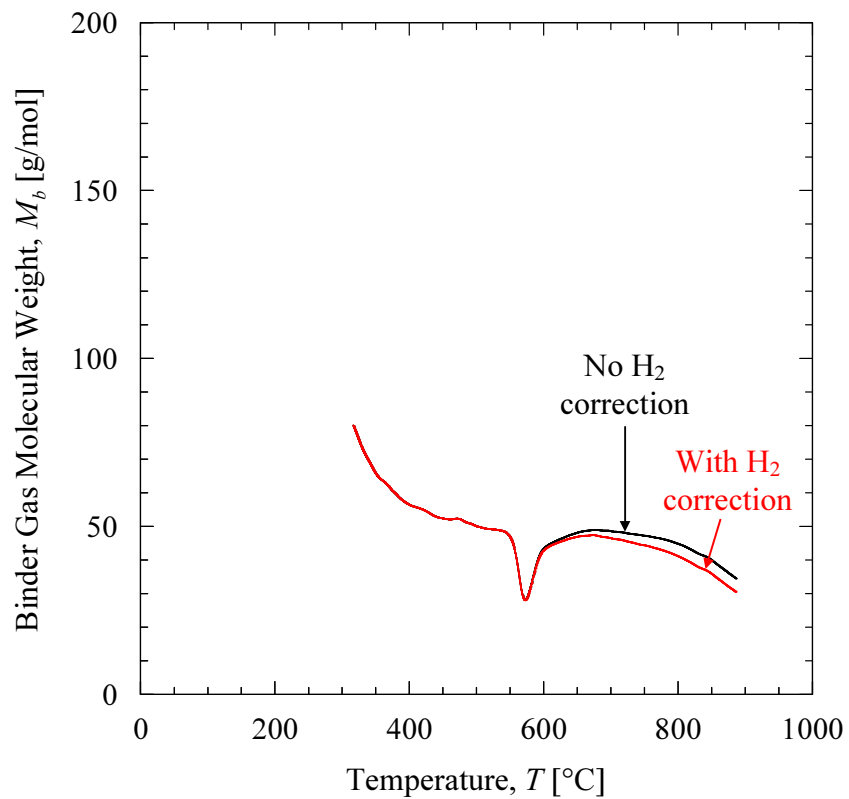


Figure 29: Comparison of the measured binder gas molecular weight as a function of temperature with and without the hydrogen dissolution correction during heating of a 0.637 g PUNB bonded sand sample at a rate of 2°C/min.

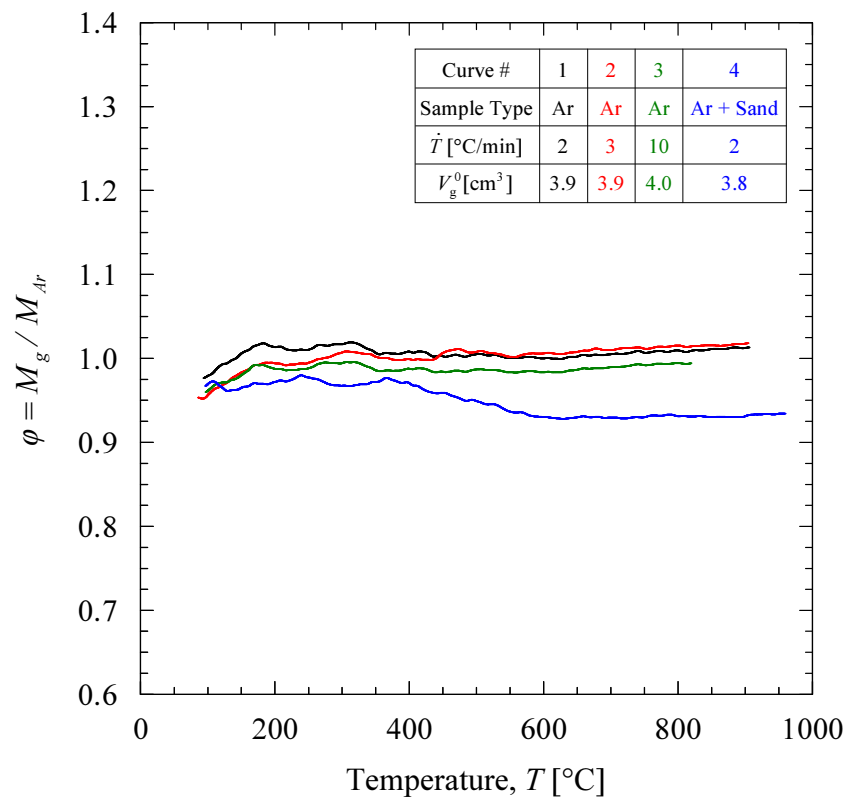


Figure 30: Comparison of the measured to known molecular weight ratio of argon for pure argon gas samples and argon gas with a 1.018 g sample of cleaned IC55 silica sand as a function of temperature during heating. The decrease in ϕ for the argon and sand test between 400°C and 600°C indicates that a small amount of gas is generated from sand decomposition.

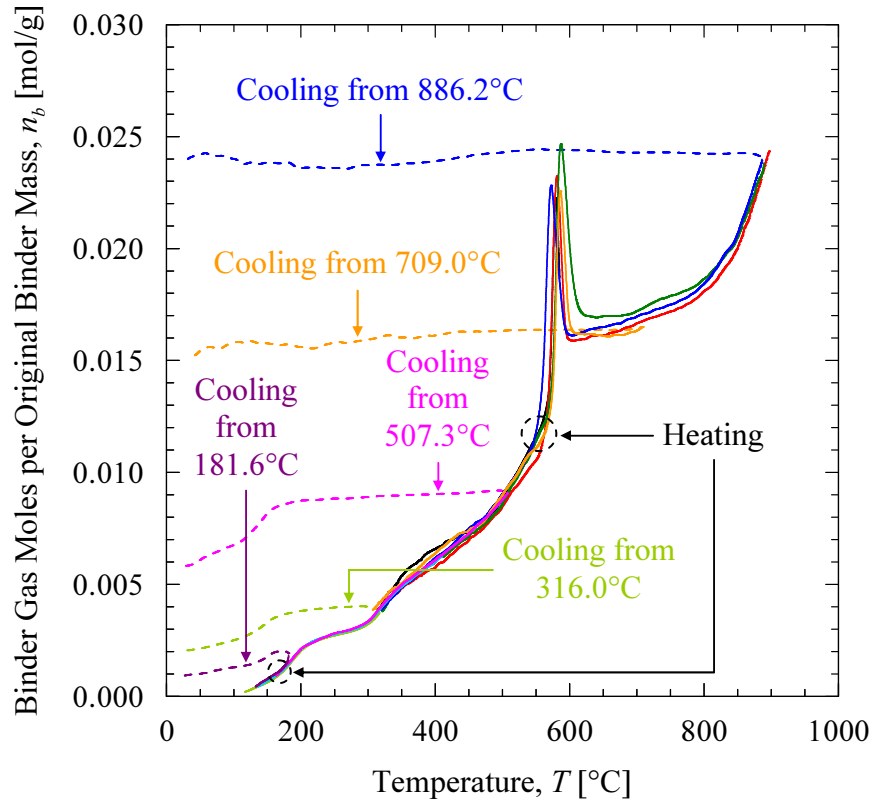


Figure 31: Measured binder gas moles evolved per original binder mass as a function of temperature during heating and cooling of different PUNB bonded sand sample masses. The color scheme of the curves follows that of Figure 27. The heating rate is 2°C/min, and a significant decrease in n_b during cooling indicates condensation of the binder gas.

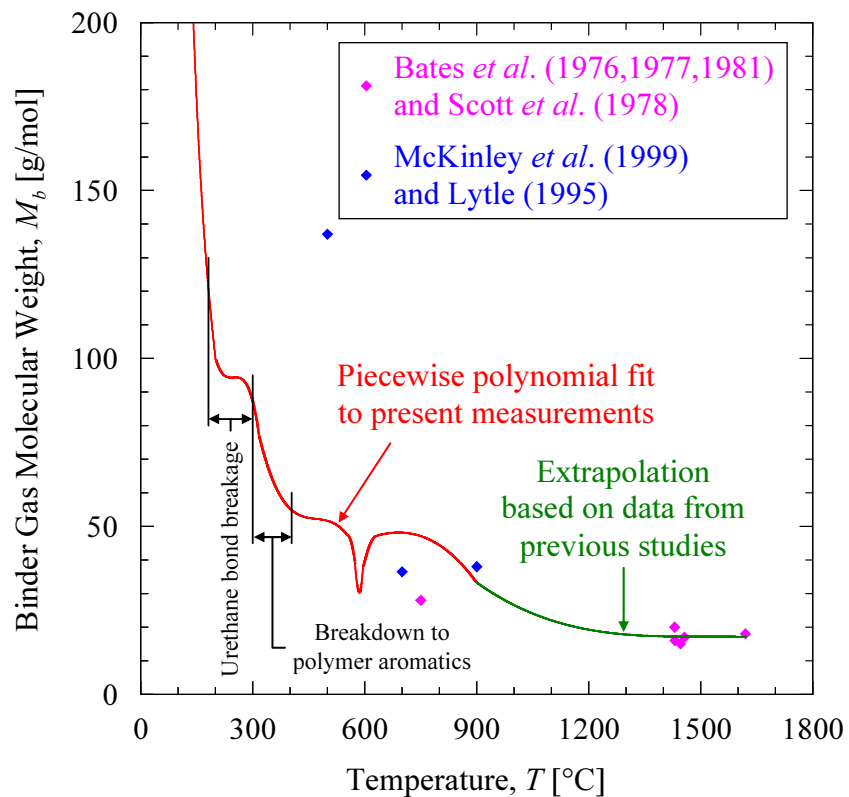


Figure 32: Comparison of the piecewise polynomial fitted to the present binder gas molecular weight measurements for a heating rate of $2^{\circ}\text{C}/\text{min}$ with the results from previous studies as a function of temperature. The data fit is extrapolated based on the average molecular weights calculated from the data of Bates *et al.* [17-19] and Scott *et al.* [20] within 2 minutes after pouring. The fitted results are also compared with the binder gas molecular weights calculated from the data of McKinley *et al.* [22] and Lytle [23]. The partial thermal degradation mechanism for a 60:40 ratio pure PUNB binder sample heated at a rate of $10^{\circ}\text{C}/\text{min}$ from Giese *et al.* [39] is superimposed on the data fit.

Table 6: Piecewise polynomial fitted to the binder gas molecular weight measurements obtained during heating of PUNB bonded sand samples at a rate of 2°C/min.

Binder Gas Molecular Weight, M_b [g/mol]	Temperature, T [°C]
$-8.638T + 1368$	$T \leq 132$
$-1.638 \times 10^{-4} T^3 + 9.988 \times 10^{-2} T^2 - 21.31T + 1677$	$132 < T \leq 200$
$-5.397 \times 10^{-5} T^3 + 4.001 \times 10^{-2} T^2 - 9.880T + 907.0$	$200 < T \leq 316$
$-6.447 \times 10^{-6} T^3 + 9.056 \times 10^{-3} T^2 - 4.253T + 720.0$	$316 < T \leq 551$
$-2.945 \times 10^{-5} T^3 + 3.230 \times 10^{-2} T^2 - 8.768T - 1.100$	$551 < T \leq 574$
$1.197 \times 10^{-4} T^3 - 0.1401T^2 + 41.04T + 3.500$	$574 < T \leq 595$
$-1.090 \times 10^{-5} T^3 + 1.367 \times 10^{-2} T^2 - 4.211T + 0.000$	$595 < T \leq 635$
$-2.680 \times 10^{-7} T^3 + 2.681 \times 10^{-4} T^2 + 1.269 \times 10^{-2} T - 0.1900$	$635 < T \leq 898$
$-7.139 \times 10^{-8} T^3 + 3.233 \times 10^{-4} T^2 - 0.4878T + 262.4^*$	$T > 898$

*Extrapolated based on the molecular weights calculated from Bates *et al.* [17-19] and Scott *et al.* [20]

CHAPTER 5. CONCLUSIONS

The present measurements reveal the complex nature of the gas evolution from PUNB bonded sand during heating and cooling. Available temperature-resolved binder gas evolution data that correspond to conditions experienced during casting processes are extremely limited, and the present work greatly expands upon the current knowledge of binder gas evolution behavior.

The present TGA measurements show that the PUNB binder significantly decomposes when heated to elevated temperatures. It is also found that the binder gas mass evolution from PUNB bonded sand is not strongly influenced by the heating rate. Fairly good agreement exists between the present binder gas mass evolution measurements for a gas flow rate of 80 cm³/min and the measurements from previous studies. However, the purge gas flow rate employed during TGA is found to influence the bonded sand decomposition behavior, and care must be taken when comparisons are made between TGA measurements of bonded sand performed using different purge gas flow rates.

The gas measurement apparatus developed in the present study is used to accurately measure the molecular weight of the gas evolved from PUNB bonded sand as a function of temperature. For a heating rate of 2°C/min, it is found that the PUNB binder gas molecular weight generally decreases from 375 g/mol at 115°C to 33.3 g/mol at 898°C. The present molecular weight measurements are consistent with the molecular weights calculated using the binder gas composition data from previous studies. The binder gas components do not condense during cooling when the bonded sand is heated above 709°C. However, if the bonded sand is heated to temperatures below 507°C, some of the binder gas components will condense during cooling at approximately 165°C. It is also speculated that the present measurements and high temperature extrapolation may be used to approximate the molecular weight of the gas evolved from PUCB or PUNB bonded sand for heating rates between 2°C/min and 100°C/min.

While the data from the present binder gas evolution measurements may be readily used with current binder gas evolution models, additional research is needed. The binder gas mass and molecular weight must be measured for heating rates greater than $100^{\circ}\text{C}/\text{min}$ in order to fully describe the binder gas evolution at distances less than 0.5 in from the mold-metal interface. The exact cause of the peak in the measured binder gas molecular weight at 585°C during heating is unknown, and additional experiments are needed to investigate the gas evolution behavior near 585°C . The continuous variation in the binder gas molecular weight below 115°C and above 898°C is still experimentally undetermined. The binder decomposition reactions are kinetic in nature, and the gas evolution during heating and holding of bonded sand at elevated temperatures is most likely very different from the bonded sand gas evolution during heating only. Therefore, the binder gas evolution experienced during heating and holding of bonded sand at elevated temperatures needs to be explored. The influence of cooling on binder gas evolution deserves greater attention, and complete knowledge of the binder gas evolution during heating and cooling will provide the means to describe the gas evolution in bonded sand molds and cores during the entire casting process. While the techniques for measuring the binder gas composition are not well suited for determining the binder gas molecular weight as a function of temperature, it is still important to know the composition of the gas evolved from bonded sand. Additional study to determine the binder gas composition as a function of temperature would be highly valuable.

The number of factors that influence the evolution of gas from bonded sand molds and cores is more than a single study can explore. The goal of this research was to obtain a better understanding of the binder gas mass evolution and molecular weight under conditions similar to those experienced during sand casting processes. Future studies could employ the present experimental techniques to determine the effects of different heating ranges, binder systems, binder compositions, sand types, sand coatings, and sand additives on the evolution of the binder gas.

REFERENCES

1. Campbell, J., *Castings*, 2nd ed, pp. 99-116, Butterworth-Heinemann, Oxford, United Kingdom (2003).
2. Rahmoeller, K.M., "Mold Binder Decomposition: Prime Source of Cast Iron Defects Part 4 of 4," *Modern Casting*, vol. 83, no. 10, pp. 36-39 (1993).
3. Bates, C.E., and Burch, R., "Core and Mold Gas Evolution: Porosity in Castings," *Foundry Management & Technology*, vol. 135, no. 5, pp. 17-18 (2007).
4. Gibbs, S., "Illuminating Core Gas," *Modern Casting*, vol. 98, no. 10, pp. 34-37 (2008).
5. Worman, R.A., Nieman, J.R., "A Mathematical System for Exercising Preventive Control over Core Gas Defects in Gray Iron Castings," *AFS Transactions*, vol. 81, pp. 170-179 (1973).
6. Levelink, H.G., Julien, F.P.M.A., De Man, H.C.J., "Gas Evolution in Molds and Cores as the Cause of Casting Defects," *AFS International Cast Metals Journal*, vol. 6, pp. 56-63 (March 1981).
7. Naro, R.L., Pelfrey, R.L., "Gas Evolution of Synthetic Core Binders: Relationship to Casting Blowhole Defects," *AFS Transactions*, vol. 91, pp. 365-376 (1983).
8. Naro, R.L., "Porosity Defects in Iron Castings from Mold-Metal Interface Reactions," *AFS Transactions*, vol. 107, pp. 839-851 (1999).
9. Monroe, R., "Porosity in Castings," *AFS Transactions*, vol. 113, pp. 519-546 (2005).
10. Rogers, C., "Numerical Mold and Core Sand Simulation," in *Modeling of Casting, Welding, and Advanced Solidification Processes – X*, eds. D.M. Stefanescu, J.A. Warren, M.R. Jolly, and M.J.M. Krane, TMS, Warrendale, PA, 2003, pp. 625-632.
11. Kimatsuka, A., Ohnaka, I., Zhu, J.D., Sugiyama, A., and Kuroki, Y., "Mold Filling Simulation for Predicting Gas Porosity," in *Modeling of Casting, Welding and Advanced Solidification Processes – XI*, eds. C.A. Gandin and M. Bellet, TMS, Warrendale, PA, 2006, pp. 603-610.
12. Starobin, A., Hirt, C.W., and Goettsch, D., "A Model for Binder Gas Generation and Transport in Sand Cores and Molds," in *Modeling of Casting, Welding and Advanced Solidification Processes – XII*, eds. S.L. Cockcroft and D.M. Maijer, TMS, Warrendale, PA, 2009, pp. 345-352.
13. Trinowski, D.M., "Foundry," in *Phenolic Resins: A Century of Progress*, ed. L. Pilato, pp. 451-502, Springer, New York, NY (2010).
14. Naro, R.L. and Hart, J.F., "Phenolic Urethane No-Bake Binders: Ten Years of Progress," *AFS Transactions*, vol. 88, pp. 57-66 (1980).
15. Carey, P.R., Sturtz, G., "Sand Binder Systems Part IV – Urethane Binders (Continued)," *Foundry Management & Technology*, vol. 123, no. 6, pp. 25-29 (1995).

16. Carey, P.R., Archibald, J., "Sand Binder Systems Part X – The Phenolic Urethane Amine Cold Box System," *Foundry Management & Technology*, vol. 123, no. 12, pp. 21-26 (1995).
17. Bates, C.E. and Scott, W.D., "The Decomposition of Resin Binders and the Relationship Between Gases Formed and the Casting Surface Quality Part 2 – Gray Iron," *AFS Transactions*, vol. 84, pp. 793-804 (1976).
18. Bates, C.E. and Scott, W.D., "Decomposition of Resin Binders and the Relationship Between the Gases Formed and the Casting Surface Quality – Part 3," *AFS Transactions*, vol. 85, pp. 209-226 (1977).
19. Bates, C.E. and Monroe, R.W., "Mold Binder Decomposition and Its Relation to Gas Defects in Castings," *AFS Transactions*, vol. 89, pp. 671-686 (1981).
20. Scott, W.D., Goodman, P.A., and Monroe, R.W., "Gas Generation at the Mold-Metal Interface," *AFS Transactions*, vol. 86, pp. 599-610 (1978).
21. Monroe, R., Steel Founder's Society of America, Crystal Lake, IL, private communication, 2011.
22. McKinley, M.D., Lytle, C.A., and Bertsch, W., "Pyrolysis of Core Resins Used in Metalcasting," *AFS Transactions*, vol. 107, pp. 407-412 (1999).
23. Lytle, C.A., "Analysis of Volatiles from Foundry Resin Binder Systems," Master's Thesis, University of Alabama, Tuscaloosa, AL (1997).
24. Wang, Y., Cannon, F.S., Salama, M., Fonseca, D.A., and Giese, S., "Characterization of Pyrolysis Products from a Biodiesel Phenolic Urethane Binder," *Environmental Science & Technology*, DOI: 10.1021/ES8024929, <http://pubs.acs.org/journal/esthag> (2009).
25. Dietert, H.W., Graham, A.L., Praski, R.M., "Gas Evolution in Foundry Materials – Its Source and Measurement," *AFS Transactions*, vol. 84, pp. 221-228 (1976).
26. Moore, J.J., Mason, R., "An Examination of the Gas Evolution Characteristics of Various Synthetic Core Binders," *The British Foundryman*, vol. 74, no. 9, pp. 189-195 (1981).
27. Zhang, B., Garro, M., Chautard, D., Tagliano, C., "Gas Evolution from Resin-Bonded Sand Cores Prepared by Various Processes," *Metallurgical Science and Technology*, vol. 20 no. 2, pp. 27-32, (2002).
28. Scarber, P., Bates, C.E., Griffin, J., "Effects of Mold and Binder Formulations on Gas Evolution When Pouring Aluminum Castings," *AFS Transactions*, vol. 114, pp. 435-445 (2006).
29. Winardi, L., Littleton, H.E., Bates, C.E., "Gas Pressures in Sand Cores," *AFS Transactions*, vol. 115, pp. 303-312 (2007).
30. Winardi, L., Griffin, R.D., Littleton, H.E., Griffin, J.A., "Variables Affecting Gas Evolution Rates and Volumes from Cores in Contact with Molten Metal," *AFS Transactions*, vol. 116, pp. 505-521 (2008).

31. Ridsdale & Company, Ltd., "AFS Foundry Sand Testing Equipment Operating Instructions," obtained from http://www.basrid.co.uk/AFS_OIM.pdf, pp. 115-120.
32. Thole, J. and Beckermann, C., "Measurement of Elastic Modulus of PUNB Bonded Sand as a Function of Temperature," *International Journal of Metalcasting*, vol. 4, no. 4, pp. 7-18 (2010).
33. DASyLab[®] v8.0, National Instruments, 11500 N. Mopac Expwy, Austin, TX 78759.
34. Incropera, F.P., DeWitt, D.P., Bergman, T.L., Lavine, A.S., *Fundamentals of Heat and Mass Transfer*, 6th edition, pp. 563-564, John Wiley & Sons, Inc., Hoboken, NJ (2007).
35. Munson, B.R., Young, D.F., Okiishi, T.H., and Huebsch, W.W., *Fundamentals of Fluid Mechanics*, 6th edition, pp. 50-53, John Wiley & Sons, Inc., Hoboken, NJ (2009).
36. Moran, M.J., Shapiro, H.N., Boettner, D.D., and Bailey, M.B., *Fundamentals of Engineering Thermodynamics*, 7th edition, pp. 706-711, John Wiley & Sons, Inc., Hoboken, NJ (2010).
37. Vargaftik, N.B., Filippov, L.P., Tarzimanov, A.A., and Totskii, E.E. *Handbook of Thermal Conductivity of Liquids and Gases*, pp. 16-48, CRC Press, Boca Raton, FL (1994).
38. Peters, F., Voigt, R., Ou, S.Z., and Beckermann, C. "Effect of Mould Expansion on Pattern Allowances in Sand Casting of Steel," *International Journal of Cast Metals Research*, vol. 20, no. 5, pp. 275-287 (2007).
39. Giese, S.R., Roorda, S.C., and Patterson, M.A., "Thermal Analysis of Phenolic Urethane Binder and Correlated Properties," *AFS Transactions*, vol. 117, pp. 355-366 (2009).